Review

Catalytic Oxidation Processes for the Upgrading of Terpenes: State-of-the-Art and Future Trends

Audrey Denicourt-Nowicki [1,*], Mariem Rauchdi [1,2], Mustapha Ait Ali [2] and Alain Roucoux [1]

[1] Ecole Nationale Supérieure de Chimie de Rennes, CNRS, ISCR-UMR 6226, F-35000 Rennes, France; rauchdimariem@gmail.com (M.R.); alain.roucoux@ensc-rennes.fr (A.R.)

[2] Equipe de Chimie de Coordination et de Catalyse, Département de Chimie, Faculté des Sciences Semlalia, Université Cadi Ayyad, BP 2390 Marrakech, Morocco; aitali@uca.ac.ma

* Correspondence: Audrey.Denicourt@ensc-rennes.fr

check for updates

Abstract: Terpenic olefins constitute a relevant platform of renewable molecules, which could be used as key intermediates for the perfumery, flavoring, and pharmaceutical industries. The upgrading of these cheap and available agro-resources through catalytic oxidation processes remains of great interest, leading to the formation of either epoxides via the oxidation of the olefinic bond or α,β-unsaturated ketones by the Csp^3-H functionalization at the α-position of the double bond. This critical review summarizes some of the most relevant homogeneous or heterogeneous catalysts designed for the oxidation of some abundant terpenic olefins in the last decade (2008–2018).

Keywords: terpenes; catalysts; epoxidation; allylic oxidation; sustainable chemistry

---

1. Introduction

Monoterpenes based on a 10-carbons skeleton and sesquiterpenes with 15 carbons are highly abundant renewables, present as major constituents in essential oils and natural resins or as co-products from the paper and citric juice industries. In 2015, the world production of turpentine oils was estimated around 360,000 tons, arising from coniferous trees or as a co-product of the paper industry. Turpentine can then be distillated to afford its major constituents, α- and β-pinene [1]. Besides, limonene is principally obtained as a byproduct of the citric fruit juice industry, with a worldwide production of more than 70,000 tons [2]. Terpenes constitute a sustainable platform of cheap renewables that could be converted into valuable products for the production of perfumes, flavors, or pharmaceuticals, as well as pertinent and potentially optically active building blocks [3,4]. The upgrading of terpenes can involve many synthetic transformations, such as isomerization, hydrogenation, oxidation, rearrangement, or esterification [5,6]. On this topic, Golets and Mikkola published in 2015 an exhaustive review of scientific advances for α-pinene valorization, including various catalytic applications (such as isomerization, hydrogenation, acetoxylation, etc.) [7]. Among these reactions, the oxyfunctionalization of terpenic olefins through oxidation processes remains a relevant synthetic methodology to afford either epoxides or allylic ketones and alcohols (Figure 1). In the context of an eco-responsible chemistry [8], the use of catalytic processes for their upgrading remains attractive to limit the environmental impact by lowering the energy barriers and minimizing the formation of co-products, thus simplifying the work-up [9]. In 2009, Bicas et al. reviewed various methods for terpene oxidation via microbial biotransformation using either purified enzymes or integer cells [10]. Here, we summarize some of the most relevant molecular complexes and heterogeneous catalysts designed for the oxidation of some abundant terpenic olefins, such as pinenes, limonene, valencene, or carenes, within the period of ca. 2008–2018.
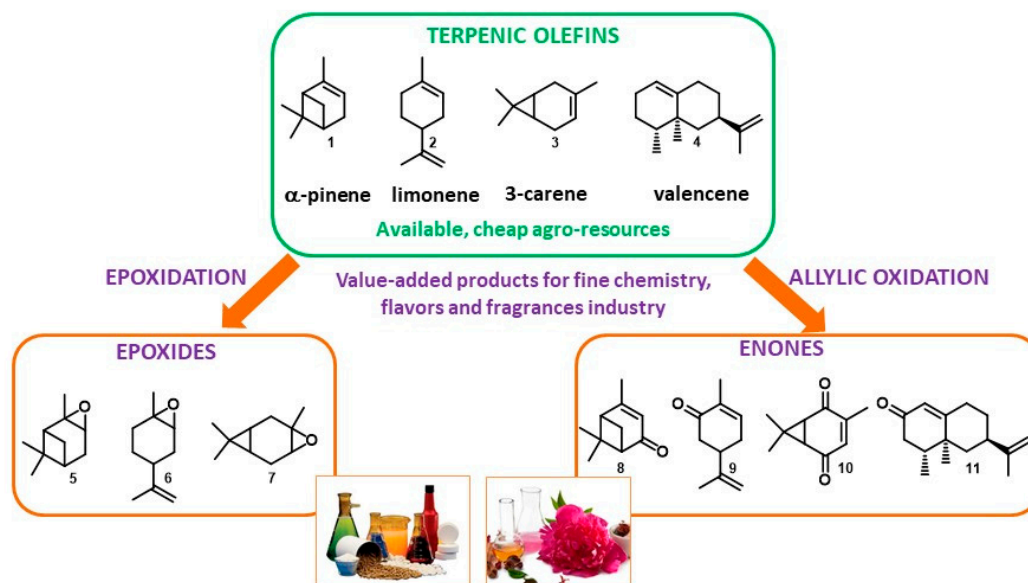
Figure 1. Oxyfunctionalization of terpenic olefins into value-added products.

One of the main challenges in these oxidation processes that should be underlined is the high control of the selectivity. In fact, complex reaction mixtures are often obtained, as realistically illustrated in the literature by Antunes and coworkers for the catalytic oxidation of α-pinene **1** using H_2O_2 as the oxidant and the biomimetic [Fe^{III}(BPMP)Cl(μ-O)$Fe^{III}Cl_3$] catalyst to methane monooxygenase (MMO) enzymes [11]. Although efficient catalytic activities with high conversions into the allylic products were achieved, the chromatogram (Figure 2) showed the complexity of the crude reaction mixture, with more than 20 products detected. This result fully justifies the development of new investigations to improve the selectivity with designed catalysts.
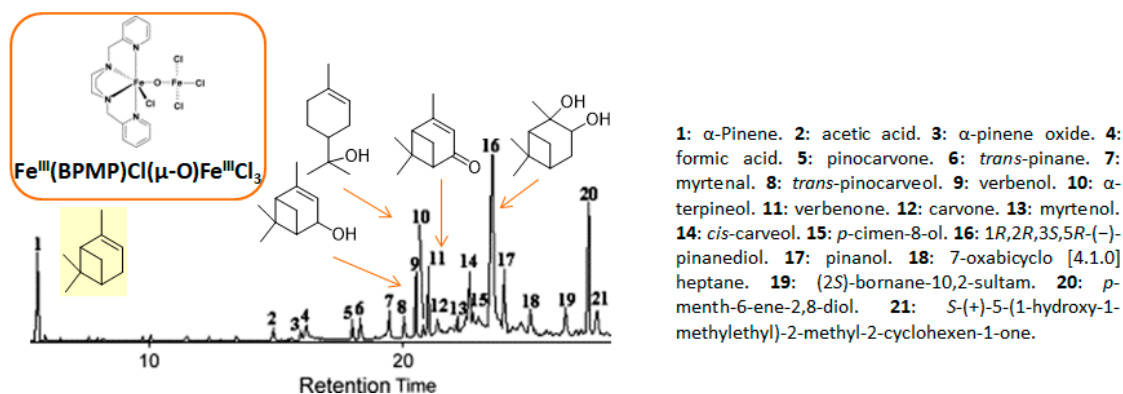

1: α-Pinene. **2**: acetic acid. **3**: α-pinene oxide. **4**: formic acid. **5**: pinocarvone. **6**: *trans*-pinane. **7**: myrtenal. **8**: *trans*-pinocarveol. **9**: verbenol. **10**: α-terpineol. **11**: verbenone. **12**: carvone. **13**: myrtenol. **14**: *cis*-carveol. **15**: *p*-cimen-8-ol. **16**: 1*R*,2*R*,3*S*,5*R*-(−)-pinanediol. **17**: pinanol. **18**: 7-oxabicyclo [4.1.0] heptane. **19**: (2*S*)-bornane-10,2-sultam. **20**: *p*-menth-6-ene-2,8-diol. **21**: *S*-(+)-5-(1-hydroxy-1-methylethyl)-2-methyl-2-cyclohexen-1-one.

Figure 2. Chromatogram of the challenging α-pinene oxidation with [Fe^{III}(BPMP)Cl(μ-O)$Fe^{III}Cl_3$] (adapted from reference [11]).

The selectivity could in some cases be substrate-dependent, as observed by Gusevskaya's team with chromium-containing mesoporous molecular sieves MCM-41 prepared by a sol-gel method with tetraethoxysilane and $CrCl_3 \cdot 6H_2O$ [12]. While the solvent-free oxidation of β-pinene **12**, using molecular oxygen, afforded almost exclusively allylic mono-oxygenated derivatives, α-pinene **1** and limonene **2** were transformed into both epoxides and allylic oxidation products (Figure 3). These observations point out the difficulties in obtaining a general procedure for the oxidation of terpenes with a unique catalyst.
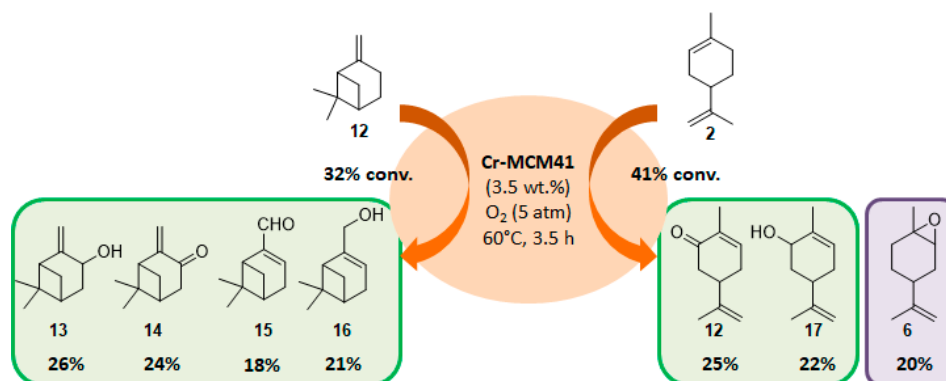
Figure 3. Solvent-free oxidation of terpenic olefins using Cr-MCM41 catalyst (adapted from reference [12]).

2. Epoxidation of Terpenes

Epoxidation reactions constitute great synthetic transformations of olefins into epoxides and *cis*-diols [13], as versatile intermediates for various areas from material science to bulk chemicals [14]. In the last decades, many efforts have been devoted to reducing the environmental footprint of these processes. The main challenges rely on the use of benign and abundant metals instead of scarce and potentially toxic metals (chromium or osmium) and more atom-economic oxidants such as dioxygen or hydrogen peroxide. Some recent examples of molecular complexes and heterogeneous catalysts are presented hereafter, arbitrary classified in three metal groups: (i) noble and semi-noble metals, (ii) first row metals, and (iii) miscellaneous metals.

2.1. Using Homogeneous Complexes

2.1.1. Noble and Semi-Noble Metals

In this subsection, among the short list of chemically noble metals (Pd, Rh, Ru, Au, Ag, Pt, Ir, Os) that almost all chemists agree, semi-noble metals such as rhenium (Re) will be included.

Palladium catalysts. Oxidation of olefins by dioxygen, using Wacker-type systems (PdCl$_2$/CuCl$_2$), is quite limited, owing to the formation of many co-products due to the Lewis acidity of CuCl$_2$ [15]. Alternatively, da Silva et al. designed a CuCl$_2$-free oxidative process based on a PdCl$_2$/H$_2$O$_2$/CH$_3$CN combination [16] that could improve the selectivity toward oxidation products (Table 1).

Table 1. Oxidation of camphene **18** catalyzed by palladium salts [a] (adapted from reference [16]).

Entry	PdCl$_2$ (mmol)	Initial H$_2$O$_2$ (mmol)	Conv. into Oxidation Products [b] (%)	Conv. into Other Products [b,c] (%)	Selectivity [b] (%)		
					19	**20** [d]	**21**
1 [e]	0	3.0	10	8	10	-	-
2	0.1	1.5	32	8	90	5	5
3	0.1	3.0	78	15	8	49	43
4	0.1	6.0	60	27	5	35	60
5 [f]	0.3	3.0	86	11	2	67	31
6 [f]	0.4	3.0	90	10	3	64	33

[a] Reaction conditions: Camphene (2.5 mmol), H$_2$O$_2$, 60 °C, CH$_3$CN (10 mL), 12 h. [b] Determined by GC analyses. [c] Complex mixture of products resulting from hydration of the olefinic bond, the skeletal rearrangement (hydroxycamphene, borneol, tricyclene). [d] **20** determined as two isomers in a 3:1 proportion. [e] Blank experiment: no PdCl$_2$, 3 mmol H$_2$O$_2$, 6 h. [f] Conversion reached after 6 h reaction.

First, a blank test on camphene **18** without catalyst afforded only 10% of epoxide **19** in 6 h, in standard conditions (Table 1, Entry 1). Palladium dichloride (PdCl$_2$) gives oxidation products identified as epoxide **19**, glycol **20** (*endo* and *exo* isomers in a 3:1 proportion), and aldehyde **21** (Table 1,

Entries 2–6). Moreover, the oxidant concentration (Entries 2–4) has an impact on the conversion and the product distribution at a same Pd concentration. An optimum conversion of 78% into oxidation products was achieved with an H_2O_2/Substrate ratio of 1.2 (Entry 3) favoring the camphene-2,10-glycol **20**. This compound results either from the ring opening of **19** or from a possible hydroxypalladation of olefin in a π-camphene–palladium complex followed by heterolysis of a carbon–palladium σ-bond (Scheme 1). Moreover, higher metal concentration with an H_2O_2/substrate ratio of 1.2 (Entries 3, 5, and 6) leads to an improved conversion rate (up to 90%) and an increased selectivity toward the glycol camphene **20**. The authors proposed a pathway, based on the previous work of Gusevskaya and coworkers [15], to explain the various products formed and presumed that palladium hydroperoxidic species (ClPdOOH and/or HOPdOOH) are likely to be the active species (Scheme 1).
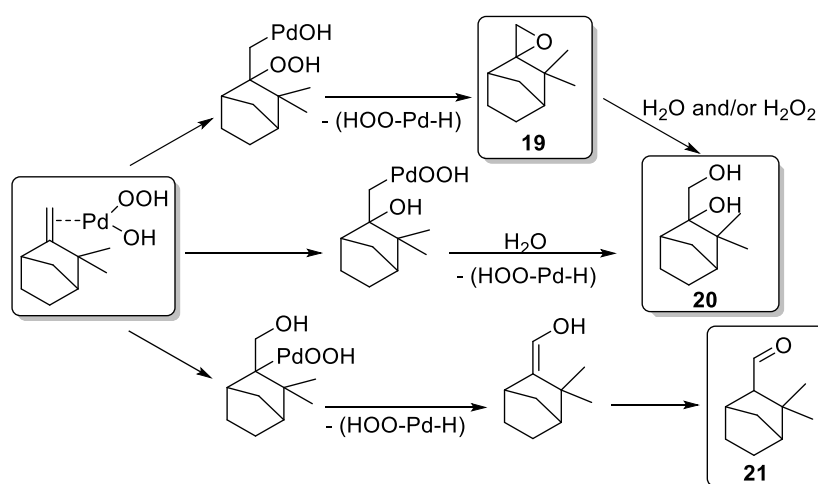
Scheme 1. Potential reaction pathways for Pd-catalyzed oxidation (adapted from reference [16]).
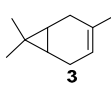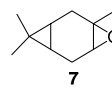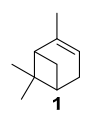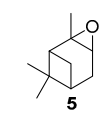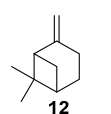
Rhenium catalyst. Methyltrioxorhenium(VII) (CH_3ReO_3, MTO) is known as a relevant oxidation catalyst, being available, stable in air (O_2 and humidity), and soluble in various solvents (even in water). In 2010, Yamazaki developed a relevant procedure for the production of terpenic epoxides with excellent yields (Table 2) using MTO as catalyst combined with 3-m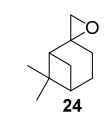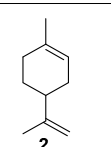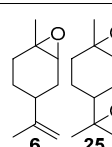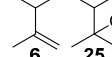ethylpyrazole and 1-methyl imidazole [17]. These additives seem relevant to avoid the ring opening and the rearrangement of acid-sensitive epoxides [18]. However, according to the substrate, the reaction conditions are quite different and the rationalization remains difficult. Both isomers of carene **3** and **22** (Entries 1–6) and pinene **1** and **12** (Entries 7–8) gave excellent yields into the corresponding epoxides, either under solventless conditions or in dichloromethane (Entries 5–6) without significant differences between both additives (Entries 3–4). However, in the case of 2-carene **22**, a lower yield was observed without 1-methylimidazole, owing to a decomposition of the epoxide under longer reaction times (Entry 2). Limonene **2** was oxidized into 1,2-epoxide **6** as the main product, along with diepoxide **25**. The use of an excess of oxidant, as well as a prolonged reaction time, selectively afforded diepoxide **25** (Entry 10).

Table 2. Methyltrioxorhenium(MTO)-catalyzed epoxidation of various terpenes—Optimization [a] (adapted from reference [17]).

Entry	Substrate	MTO (%)	Additive [b]	Solvent	Time (h)	Conv. (%) [c]	Epoxide	Yield (%)
1	**22**	0.2	A	- [d]	3	>99	**23**	>99
2		0.2	B	- [d]	3	98		35

Table 2. *Cont.*

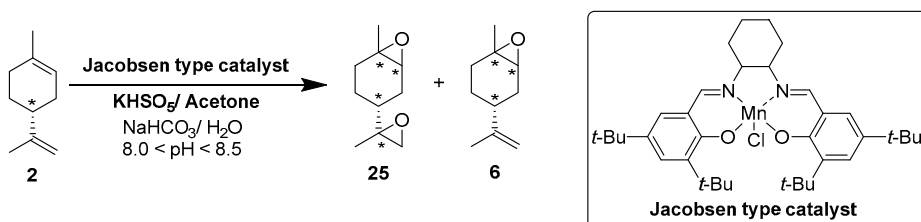| Entry	Substrate	MTO (%)	Additive [b]	Solvent	Time (h)	Conv. (%) [c]	Epoxide	Yield (%)
3		0.1	A	CH_2Cl_2	2	>99		>99
4		0.1	B	CH_2Cl_2	2	>99		99
5	**3**	0.3 [e]	A	- [d]	6	>99	**7**	>99
6		0.2	A	CH_2Cl_2	2.5	>99		94
7	**1**	0.2	A	CH_2Cl_2	4	>99	**5**	91
8	**12**	0.2	A	CH_2Cl_2	4	>99	**24**	91
9 [f]		0.2	B	- [d]	3	97		83 [g], 14 [h]
10 [f]	**2**	0.2	B	CH_2Cl_2	8	100	**6** **25**	1 [g], 98 [h]

[a] General conditions: Olefin (10 mmol), 35% H_2O_2 (12 mmol), 10 °C. [b] Additive A: 3-methylpyrazole (1 mmol) and 1-methylimidazole (0.1 mmol). Additive B: 3-methylpyrazole (1.0 mmol). [c] Analysis by GC. Yields based on olefins used. [d] Reaction without organic solvent. [e] Addition of 0.2 mol% MTO initially, and additional MTO (0.1 mol%) after 1 h. [f] Reaction at 15 °C with 25 mmol H_2O_2. [g] 1,2-epoxide. [h] Diepoxide.

2.1.2. First-Row Metals

In the context of an eco-responsible chemistry, the use of earth-abundant and cheaper first-row transition metals (Mn, Fe, Co, Ni or Cu), also called "biometals," provides an economical alternative to noble metals. Among them, only manganese complexes have been used in epoxidation of terpenes.

Manganese catalysts. Manganese presents environmental compatibility, low toxicity [19], and moderate cost [20], being the 12th most abundant element in the Earth's crust, with a concentration about 950 g per ton [21].

In 2010, Cubillos et al. [22] developed an original epoxidation process of (*R*)-limonene **2** with Jacobsen-based manganese catalysts using in situ–generated dimethyldioxirane (DMD) produced from potassium monopersulfate ($KHSO_5$) and acetone, as oxidant. While usual oxidizing agents (NaOCl, PhIO or *m*-CPBA) lead to the oxidative degradation of the catalyst, $KHSO_5$ reacts with acetone in a slightly basic medium to afford DMD. The main products observed are the diepoxide **25** and the endocyclic epoxide **6** (Scheme 2).

Scheme 2. Epoxidation of limonene **2** with a Jacobsen-type catalyst (adapted from reference [22]).

The authors proved that the reaction conditions (such as substrate/$KHSO_5$ and acetone/substrate ratios), have an influence on the selectivity and the catalyst durability (Figure 4). Good selectivities in the diepoxides **25** and total recovery of the catalyst were observed above the stoichiometric ratio of substrate/$KHSO_5$ (Figure 4a). Moreover, low amounts of acetone are in favor of the diepoxides **25**, while higher quantities lead to the formation of endocyclic *cis*-epoxide **6** (Figure 4b).
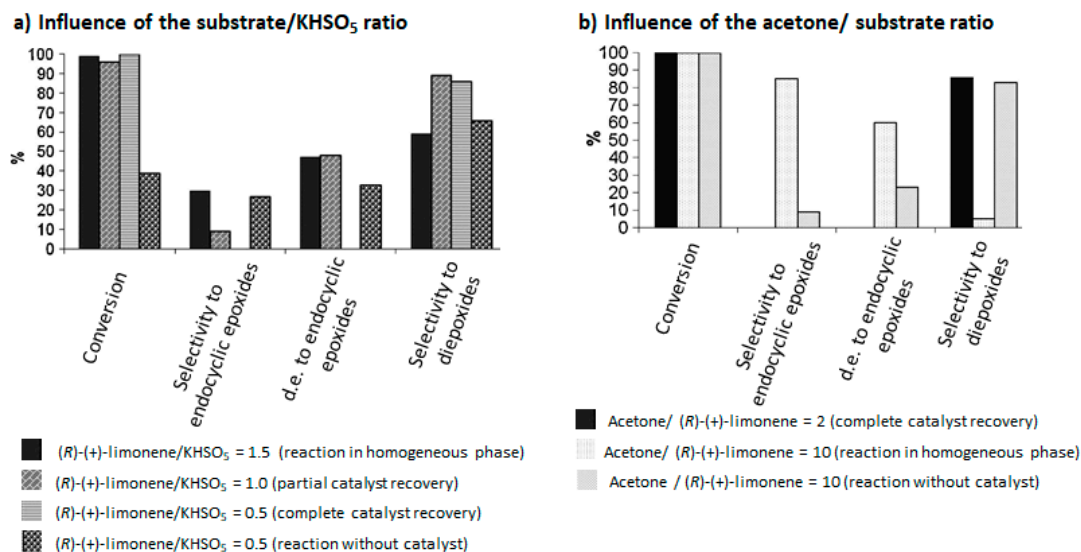
Figure 4. Influence of reaction parameters in (*R*)-(+)-limonene oxidation catalyzed by Salen manganese (III) complexes (adapted from reference [22]).

In 2012, a practical method catalyzed by a a Mn(II) salt, combined with pyridine-2-carboxylic acid (PCA) and substoichiometric butanedione, was used in the oxidation of some terpenes with H_2O_2 as oxidant [23] and proved to be particularly relevant for acid- or base-sensitive epoxide products. Under optimized reaction conditions, α-pinene **1**, 2-carene **22**, and 3-carene **3** were transformed in the corresponding epoxides, respectively **23**, **7**, and **5**, with medium to high yields and full diastereoselectivity (Figure 5). Moreover, the authors showed that this epoxide could be easily isomerized into the flavor campholenic aldehyde ingredient **26** in a one-pot procedure by a simple addition of silica at 40 °C. Mechanistic studies evidence that the catalyst uses the 3-hydroxyperoxy-3-hydroxybutan-2-one, produced in situ from reaction of butanedione with H_2O_2 as oxidant.
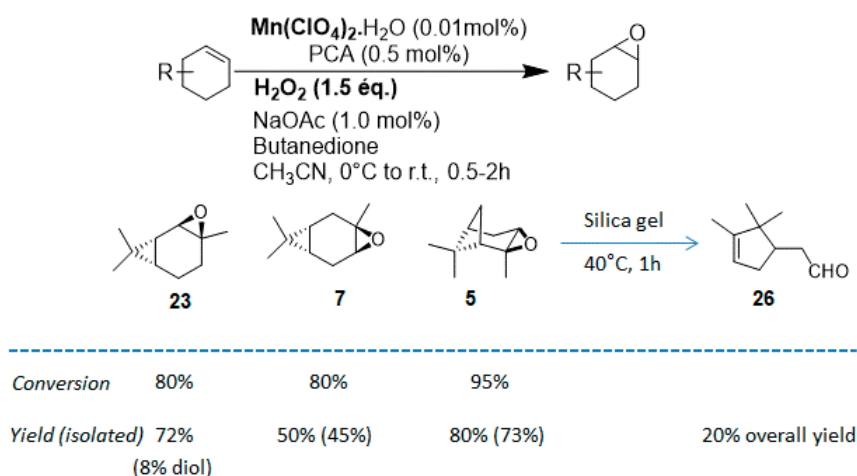
Figure 5. Oxidation of usual terpenes by an in-situ prepared Mn(II)/Pyridine-2-carboxylic acid catalyst (adapted from reference [23]).

2.1.3. Post-Transition Metals

Post-transition metals, such as gallium or aluminum, proved to be original metals for the epoxidation of terpenic olefins.

Gallium and aluminum catalysts. Recently, Shul'pin and coworkers [24] used soluble gallium nitrate salts as catalysts in the epoxidation of carvone **27** and limonene **2** with hydrogen peroxide and

compared the results to aluminum analogs. Both metals lead to a 60% conversion in 3 h at 80 °C, with a mass balance of 65%, which could be explained by the formation of other volatile products. The selectivity in internal and external epoxides **28** and **29** for both metals is given on Figure 6.
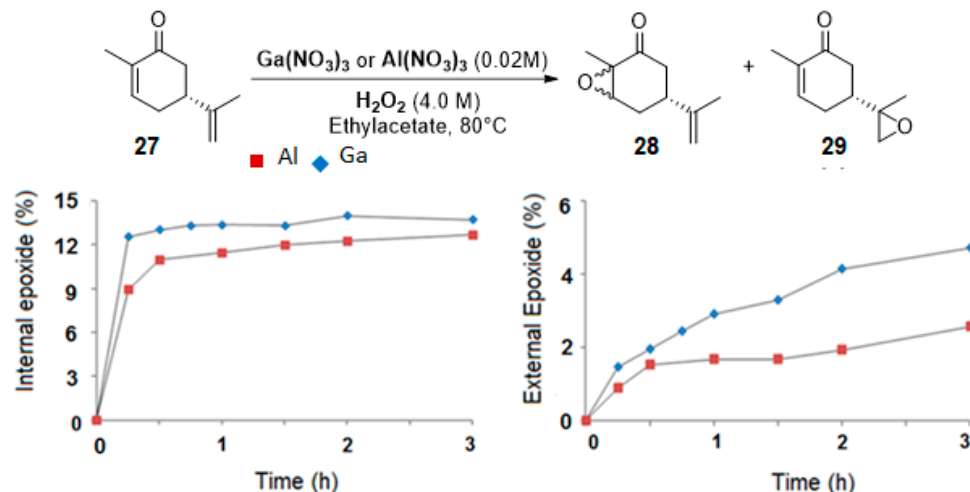
Figure 6. Epoxidation of (*R*)-carvone. Gallium vs. Aluminum salts. Conditions: Carvone (1.0 M) with H_2O_2 (4.0 M) containing 3.2 M H_2O, Catalyst (0.02 M), Ethylacetate, 80 °C (adapted from reference [24]).

Kinetic curves provide interesting mechanistic information. First, although both catalysts gave the same amount of internal epoxide **28** (ca. 13% in 3 h), radical oxygen species are formed faster with Ga^{3+} salts with regard to the yields in internal epoxide after 15 min (12% for Ga^{3+} vs. 9% for Al^{3+}). Moreover, the authors observed that, after 30 min, the yield in external epoxide **29** plateaued for Al^{3+} species but kept increasing for Ga^{3+} species. This behavior was explained by the enhanced ability of this metal to produce hydroxyl radicals, which are probably responsible for the oxidation of the external bond [25]. This hypothesis was confirmed by the addition of pyrazine-2-carboxylic acid (PCA), known as a promoter of hydroxyl radicals, and thus affording higher amount of external epoxide. This system was extended to the oxidation of limonene **2** (Scheme 3), leading to the major formation of diols **31** with quite low yields.
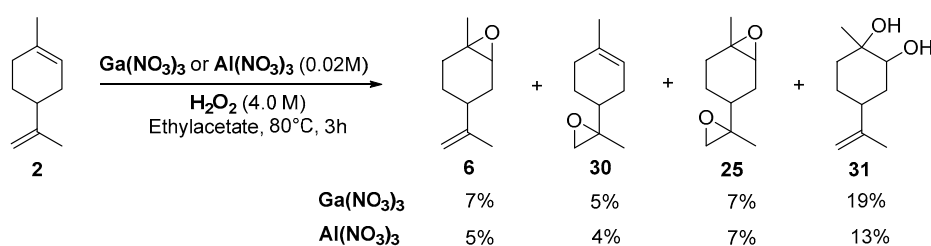
Scheme 3. Galium or Aluminum-catalyzed oxidation of limonene (adapted from reference [24]).

2.1.4. Miscellaneous Metals

Tungsten catalysts. In an original way, the epoxidation of several terpenic olefins was performed using a catalytic system based on sodium tungstate (Na_2WO_4) and $PhP(O)(OH)_2$ as co-catalyst, which coordinates the metal center to form a phosphonate complex, and [Me(*n*-C_8H_{17})$_3$N]HSO$_4$ as a phase transfer catalyst [26]. The reactions were performed in the presence of aqueous H_2O_2 as an oxidant under nearly neutral conditions. Excellent yields and selectivities were achieved toward the corresponding epoxides (Scheme 4).

Examples

	5	6	7
Yield	87%	82%	93%
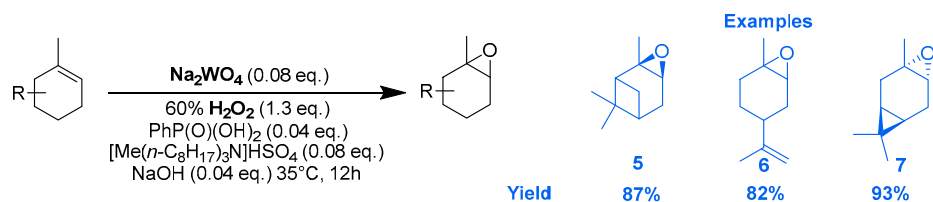
Scheme 4. Na_2WO_4-catalyzed epoxidation of olefinic terpenes (adapted from reference [26]).

2.2. Using Heterogeneous Complexes

Sustainable epoxidation reactions based on solid catalysts also remains a subject of extensive research with the aim of reducing the environmental footprint [27].

2.2.1. Transition Metal–Free Catalysts

To our knowledge, only two publications are reported in the literature concerning the epoxidation of terpenic olefins through metal-free catalysts.

In 2014, the team of Shul'pin has described for the first time the use of cheap aluminum oxide, as an efficient and selective promoter for the epoxidation of limonene **2** using green hydrogen peroxide (H_2O_2), at moderate temperature (80 °C) in ethylacetate [28]. Based on three reaction parameters such as the initial amounts of substrate, H_2O_2, and alumina, the targeted reaction was optimized to define the best conditions to achieve the most productive epoxidation reaction with regard to the initial rates of the accumulation of internal epoxide **6** as well as diepoxides **25**. Thus, by modifying the reaction conditions, the selectivity could be easily modulated (Scheme 5).
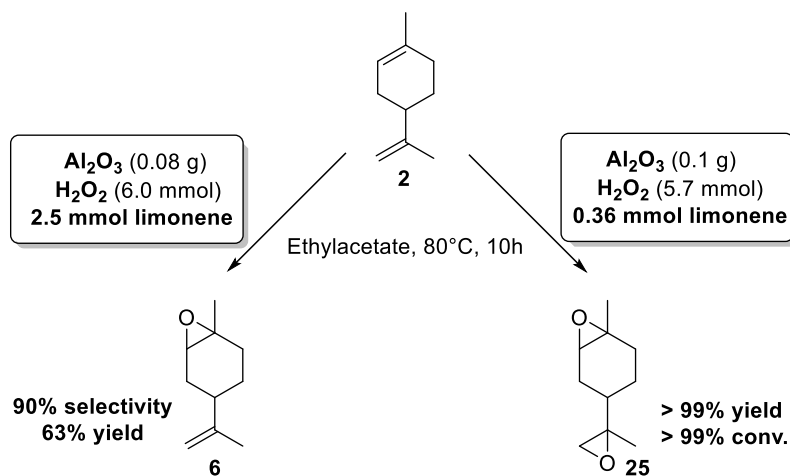
Scheme 5. Alumina-catalyzed limonene epoxidation. Internal epoxide vs. diepoxides (adapted from reference [28]).

In 2015, carbon nanotubes (CNTs) were used as metal-free catalysts for the selective epoxidation of α-pinene **1** in the presence of molecular oxygen as terminal oxidant (Table 3) [29].

Table 3. Catalytic performances of carbon nanotubes in the oxidation of α-pinene **1** [a] (adapted from reference [29]).

Entry	Catalyst	Conv. (%)	Product Selectivity [b] (%)				E/A [c] Ratio
			Epoxide 5	Verbenone 8	Verbenol 32	Verbenyl Hydroperoxide 33	
1	Blank [d]	10.3	24.5	11.7	15.0	40.4	0.9
2	CNTs	24.6	33.8	7.9	6.1	37.9	2.4
3	NCNTs [e]	54.5	37.8	14.1	17.5	15.3	1.2
4	NCNTs [f]	51.0	40.6	17.1	13.8	16.4	1.3
5	NCNTs [g]	61.4	41.1	18.7	13.4	15.9	1.3

[a] Reaction conditions: Catalyst (70 mg), α-pinene (10 mL), O_2 (15 bar), CH_3CN (20 mL), 80 °C, 4 h. [b] Determined by GC analyses using *o*-dichlorobenzene as internal standard. To determine verbenylhydroperoxide **33**, samples were analysed twice (before and after reducing the hydroperoxide to verbenol **32** with triphenylphosphine). [c] E/A ratio: molar ratio of epoxidation products (α-pinene oxide **5**) to allylic oxidation products (alcohol **32** and ketone **8**). [d] Without catalyst. [e] NCNTs (N-doped carbon nanotubes) were obtai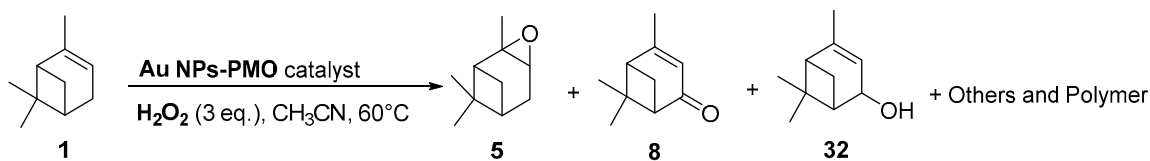ned using 100% aniline in a NH_3 atmosphere. [f] NCNTs were treated with HNO_3 and annealed at 60 °C. [g] NCNTs were treated with HNO_3 and annealed at 900 °C.

The influence of nitrogen-doping as well as post-treatments on the catalytic performances were studied and compared to a blank experiment (Entry 1). First, epoxidation product was greatly favored with carbon nanotubes (CNTs), affording a high epoxidation/allylic oxidation product ratio of 2.4 (Entry 2). Doping with nitrogen (4.36% N) improves the conversion about twofold, up to 54.5% (Entry 3), with a high selectivity in α-pinene oxide **5** (37.8%) and an improved selectivity toward allylic products and thus a lower E/A ratio. This result could be explained by the stabilization of the peroxyl and cyclohexyl radicals by nitrogen dopants. The introduction of oxygen functions via the HNO_3 treatment has a negative effect on the conversion with regard to the increased specific surface area (Entry 4). However, a post-treatment of the catalyst by annealation at 900 °C allowed increasing the conversion up to 61% with a high epoxide selectivity of 41% (Entry 5). Thus, treatments of carbon nanotubes seem to improve conversion, to the detriment of the selectivity (E/A ratio around 1).

2.2.2. Noble and Semi-Noble Metals

Noble (Au) and semi-noble (Re) metals, also used in homogeneous catalysis for epoxidation reactions of usual olefins, were also studied as pertinent heterogeneous catalysts.

Gold catalysts. In 2011, an interesting comprehensive study was reported on the influence of pore architecture and surface modification on the dispersion and the size of gold nanoparticles, as well as their catalytic performances in the epoxidation of α-pinene **1** with H_2O_2 (Table 4) [30]. A porous support with a higher pore connectivity, such as MSU with 3D-worm like pore structure, was compared to periodic mesoporous organosilica materials (PMO) with 1D-architecture. Moreover, the AuNPs@S15P-1.4 catalyst was prepared by a post-synthesis method, known to be more efficient in anchoring metal particles, and compared to other systems synthesized by a one-pot procedure (Entry 4 vs. Entries 1–3). First, without catalyst, a conversion of 11% was achieved, with a selectivity ib epoxide of about 73%. The AuNP@MSU-2.0 material, with a 3D structure and larger nanoparticles (5–20 nm), afforded lower catalytic results in terms of conversion and epoxide selectivity (Entry 1 vs. Entries 2–4), compared to 1D catalysts which possess more active sites due to their smaller sizes. Among the PMO materials with 1D pore structures (Entries 2–4), the catalyst prepared by post-synthesis method (AuNPs@S15P-1.4), presenting a better dispersion of the metallic nanospecies with smaller sizes (1.6 nm), afforded the highest epoxide selectivity. This catalyst could be retrievable with quite similar conversion, but a decrease in the selectivity due to particles aggregation.

Table 4. Oxidation of α-pinene **1** catalyzed by gold nanoparticles supported on periodic mesoporous organosilicas [a] (adapted from reference [30]).

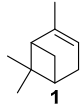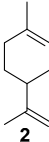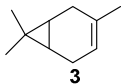| Entry	Catalyst [b]	Surface Area (m$^2\cdot$g^{-1})	Pore Size (nm)	NPs Size (nm)	Conv. [c] (%)	Selectivity (%) [c]		
						Epoxide	Allylic Oxidation Products	Others
1	AuNP@MSU-2.0	474	3.4	4.7–20	62	53	27	20
2	AuNP@M41-2.1	366	2.2	2.1	73	81	14	5
3	AuNP@S15-2.1	531	7.5	2.0	86	79	16	5
4	AuNP@S15P-1.4	329	6.3	1.6	82	95	5	-

[a] Reaction Conditions: Catalyst (50 mg or 100 mg for S15P-1.4), α-pinene (10 mmol), H$_2$O$_2$ (3 eq.), CH$_3$CN (5 mL), 8 h, 60 °C. [b] AuNP-PMO: Gold particles supported on ordered mesoporous silicas (OMS), namely MCM-41-x, MSU-x, and SBA-15-x where x is the Au loading (wt. %). [c] Determined by GC analyses.

Rhenium catalyst. Methyltrioxorhenium (CH$_3$ReO$_3$, MTO) is a well-known catalyst for oxidation reactions of a large variety of substrates, including epoxidation of olefinic compounds [31]. However, this reaction performed with hydrogen peroxide suffers from competitive reactions, such as ring-opening of the newly formed oxirane, leading to the formation of diols due to the pronounced Lewis-acidity of MTO and the production of water. The formation of these co-products could be avoided by Lewis bases acting as ligands of the metal center but used in large excess due to the low stability of the adducts and the easy oxidation of the ligands in solution [32]. In 2005, the team of Saladino solved this drawback through the microencapsulation of Lewis base adducts of MTO with cheap and easily available polystyrene (Scheme 6) [33]. This process enables to entrap the active species within the capsules of a polymeric support through non-covalent interactions. These catalysts present quite similar reactivities and selectivities, compared to their homogeneous counterparts in the epoxidation of various olefinic terpenes (α-pinene **1**, limonene **2**, and 3-carene **3**), as well as a higher stability that could facilitate the recycling. Some results are presented in Table 5.
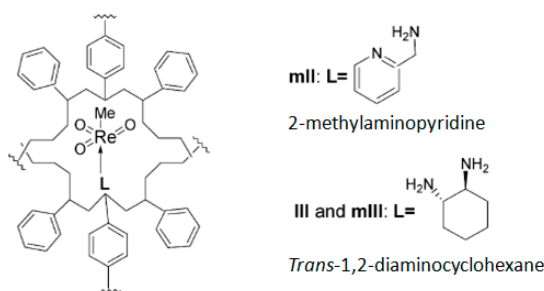
Scheme 6. Microencapsulated Lewis base adducts of methyltrioxorhenium (MTO) (adapted from reference [31]).

Table 5. Epoxidation of terpenic olefins by microencapsulated Lewis base of MTO [a] (adapted from reference [33]).

Entry	Substrate	Catalyst [b]	Time (h)	Conversion (%)	Epoxide Yield (%)
1		**III**	0.5	>98	>98
2	**1**	**mIII**	0.5	>98	>98
3		**mII**	2.0	98	98
4		**III**	1.0	95	98
5	**2**	**mIII**	2.5	96	98
6		**III**	1.0	>98	>98
7	**3**	**mIII**	1.0	>98	>98

[a] Reaction conditions: Catalyst (1% wt.), olefin (1 mmol), H_2O_2 (1.5 mmol, 35 wt. % in H_2O), 5 mL CH_3CN/CH_2Cl_2 (1/1), with a catalytic loading factor of 1.0. [b] The catalyst **III** is the homogeneous system, while **mII** and **mIII** are the microencapsulated rhenium species.

2.2.3. First-Row Metals

The anchoring of first row transition metals on inorganic or polymeric supports, as well as the design of heterogeneous analogs, was also reported in the literature.

Manganese catalysts. Schiff base complexes are well-known in olefin epoxidation [34]. However, due to their easy deactivation by oxidation and/or formation of μ-oxo dimers [35], their immobilization on solid supports seems relevant. Two examples, using either MCM-41 or SBA-15 materials, were reported in the literature for the oxidation of limonene **2**. First, Srinivas and coworkers studied the influence of the organo-functional group (propylamine, thiol or sulfonic acid) of the SBA15 support on the electronic and catalytic properties [36]. The obtained heterogeneous catalysts based on a Mn(Salen)Cl complex were compared in the aerobic oxidation of limonene **2** under mild conditions with 2-methylpropanal to facilitate the formation of Mn^{2+} ions (Table 6).

Table 6. Aerial oxidation of (*R*)-(+)-limonene **2** over "neat" and immobilized Mn(Salen)Cl complexes [a] (adapted from reference [34]).

Entry	Catalyst	Conv. [b] (%)	TOF (h⁻¹)	Selectivity (%) [b]			
				6 [c]	30 [c]	25 [c]	Allylic Oxidation Products [d]
1	"Neat" Mn(Salen)Cl	69.2	7.0	74.2	7.2	6.2	12.4
2	SBA-15-pr-NH₂-Mn(Salen)Cl	75.9	35.4	80.2	6.4	7.2	6.2
3	SBA-15-pr-SO₃H-Mn(Salen)Cl	60	17.8	82.0	8.0	2.6	7.4
4	SBA-15-pr-SH-Mn(Salen)Cl	64.1	58.9	100	0	0	0

[a] Reaction Conditions: Neat catalyst (0.0165 g) or immobilized catalyst (100 mg), limonene (3.75 mmol), 2-methylpropanal (9 mmol), air (1 bar, 2 mL.min⁻¹), toluene (20 mL), 25 °C, 8 h. [b] Determined by GC analyses. [c] Determined by Gas Chromatography and GC-MS. [d] Carvone **9** and carveol **17**.

The support functionalization allowed a relevant anchoring of the complex, compared to the "bare" one, in the following order: "bare" (0.07 mmol·g⁻¹) < sulfonic acid (0.31 mmol·g⁻¹) < thiol (0.9 mmol·g⁻¹) < amino (2.1 mmol·g⁻¹). Moreover, the metal oxidation state changed from +3 (for "neat" Mn(Salen)Cl) to +2, the extent of this reduction increasing in the following order: amino < sulfonic acid < thiol. Thus, following the variation of electron density observed in EPR and oxidizability obtained

from cyclic voltammetry experiments, the complex anchored on a propylthiol-modified SBA-15 support afforded higher catalytic activity (TOF = 58.9 h^{-1}) and complete selectivity in 1,2-epoxide **6**. However, metal leaching was detected during the reaction, thus limiting the recycling. Two years later, Vital and coworkers reported the covalent anchoring of three Salen-based manganese complexes on MCM-41 [37]. Two routes were explored: the OHPTS-DIC approach corresponds to the support functionalization with 3-chloropropyltrimethoxysilane (CIPTS), followed by its hydrolysis in hydroxyl groups, which react with 1,4-diisocyanobutane (DIC-4) and the DIC method is the direct reaction of hydroxyl groups of the complex with DIC-4. The Salen ligands bearing various diamine bridges (1,2-diamino-ethane, -cyclohexane, or -phenyl) and phenolic moieties were resumed in Scheme 7.
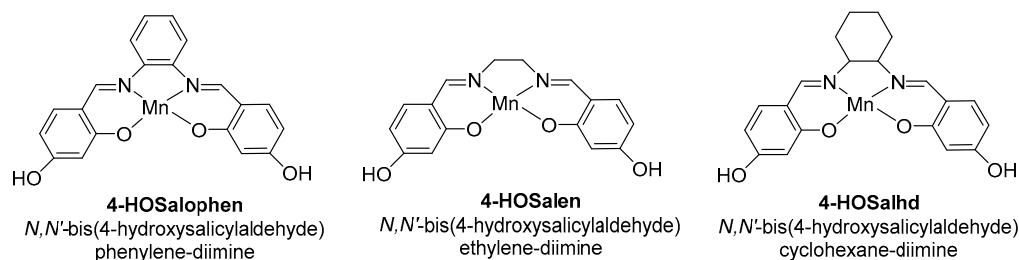
**Scheme 7.** Structure of various Mn(Salen) complexes (adapted from reference [37]).

Characterization analyses such as XPS, ICP, FTIR and TEM validate the covalent immobilization of the Mn(Salen) complex within the support, and the unchanged channel structure. Moreover, the metal content is higher in heterogeneous catalysts prepared by the OHTPS-DIC approach, and mainly located in the inner structure, as showed by XPS analyses. The obtained catalysts were evaluated in the oxidation of limonene **2** using dilute *tert*-butylhydroperoxide (*t*-BHP) as oxidant (Table 7). The reaction leads to the formation of a polymer as main product, along with limonene oxide **6** and some allylic oxidation products. Comparing the same complex (Entries 2 vs. 3 and 4 vs. 5), the catalyst prepared by the DIC method is more active (higher TOFs values) due to a lower load in organic material and thus better substrate accessibility. Finally, the catalytic activity is also very dependent on the complex used, with higher activities and selectivities toward epoxide obtained with the Mn(4-OHSalophen) complex, possessing a 1,2-diaminophenyl bridge.

Table 7. Limonene **2** oxidation catalyzed by MCM41-supported Mn(Salen) complexes [a] (adapted from reference [37]).

Entry	Complex	Method	% Mn$_{ICP}$ [b]	Conv. [c] (%)	TOF (h^{-1})	Selectivity (%) [c]		
						Limonene Oxide 6	Allylic Oxidation Products	Others
1	Mn(4-OHSalen)	OHTPS-DIC	0.21	6.0	0.4	19.5	17.8	62.7
2	Mn(4-OHSalhd)	OHTPS-DIC	5.27	80.5	1.4	2.2	3.7	94.1
3	Mn(4-OHSalhd)	DIC	1.84	51.4	1.7	3.8	2.2	93
4	Mn(4-OHSalophen)	OHTPS-DIC	0.48	84.1	14.7	10.6	6.9	82.5
5	Mn(4-OHSalophen)	DIC	0.2	60.0	17.1	10.0	8.4	81.6

[a] Reaction conditions: Catalyst (50 mg), limonene (14,5 mmol), *t*-BHP (8 eq., 3% *w/w* in acetone/*t*-butanol (100/1.2) solution), 425 mL solvent, 60 °C. [b] Mn content determined by Inductively Coupled Plasma Atomic Emission Spectroscopy (ICP-AES). [c] Determined by Gas Chromatography analyses using nonane as internal standard.

Copper catalysts. Recently, a copper-MOF catalyst was easily prepared using the 1,3,5-benzenetricarboxylate (BTC) ligand in the presence of benzoic acid as mediator, which enables to control the nucleation rate for the production of a highly crystalline material [38]. This nanoscaled [Cu$_3$(BTC)$_2$] with sizes around 390 nm proved to be efficient in epoxidation of α-pinene **1** (Scheme 8) under mild conditions (1 bar O$_2$, 40 °C) with excellent yield (>99%) and selectivity (>99%).
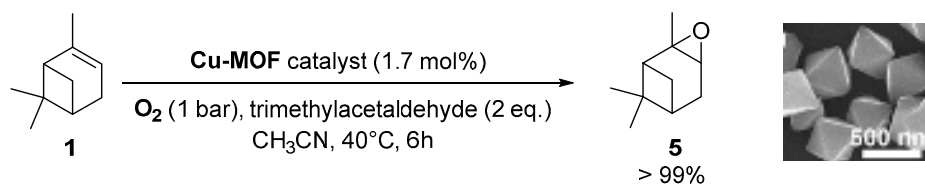
Scheme 8. Oxidation of α-pinene **1** catalyzed by nanoscaled Cu-MOF (adapted from reference [38]).

Cobalt catalysts. Based on previous work with homogeneous Co(II) complexes [39], various cobalt-exchanged zeolites were prepared by different strategies. First, these materials with various metal contents were synthesized by ion exchange of the zeolite Y support (Y) with aqueous $Co(NO_3)_2$ solution, giving NaCoYx structure with x being the cobalt content. Various alkali (K, Cs) and alkaline earth metal (Mg, Sr, and Ba) ion-containing materials were also prepared. These catalysts were evaluated in the oxidation of α-pinene **1** with molecular oxygen under optimized reaction parameters such as DMF as solvent at 100 °C (Table 8) [40].

Table 8. Oxidation of α-pinene **1** catalyzed by cobalt(III)-exchanged zeolite Y. Influence of the cobalt content and the co-cations [a] (adapted from reference [40]).

Entry	Catalyst	Chemical Composition (on Dry Basis)	Conv. [b] (%)	TOF (h^{-1})	Selectivity (%) [b]		
					Epoxide 5	Allylic Oxidation Products 8 + 32	*Trans*-Carveol 17
1	NaCoY66	$Na_{10}Co_{10}Al_{30}Si_{162}O_{384}$	32	7.2	66	28	6
2	NaCoY86	$Na_4Co_{13}Al_{30}Si_{162}O_{384}$	40	7.0	69	28	3
3	NaCoY93	$Na_2Co_{14}Al_{30}Si_{162}O_{384}$	45	7.3	71	28	1
4	NaKCoY33	$Na_{10}Co_5K_{10}Al_{30}Si_{162}O_{384}$	34	17	62	31	7
5	NaCsCoY20	$Na_6Co_3Cs_{18}Al_{30}Si_{162}O_{384}$	47	49.1	61	32	7
6	NaMgCoY33	$Na_8Co_8Mg_3Al_{30}Si_{162}O_{384}$	43	12.5	61	31	8
7	NaSrCoY33	$Na_{10}Co_5Sr_5Al_{30}Si_{162}O_{384}$	41	18.0	60	30	10
8	NaBaCoY26	$Na_{10}Co_4Ba_6Al_{30}Si_{162}O_{384}$	48	23.9	62	30	8

[a] Reaction conditions: Catalyst (300 mg), α-pinene (3 g), O_2 (5.5 bar), DMF (30 mL), 100 °C, 4 h. [b] Determined by Gas Chromatography analyses using dodecane as internal standard.

First, an increase in the metal amount (Entries 1–3) leads to higher conversions (from 32 to 45%), with a selectivity in epoxide up to 71%. Moreover, addition of alkali and alkaline earth metal ions in the zeolite structure enhances the catalytic activity (up to 48%), with a lower epoxide selectivity of 60–62%, cesium being the best candidate.

In 2014, to facilitate the catalyst's recovery, a chloromethylated polystyrene-supported cobalt(II) complex, prepared through a two-step process, was used for the aerobic epoxidation of α- and β-pinenes **1** and **12** (Figure 7) [41]. Although the reaction occurred quite easily to form the epoxide products, lower selectivities were observed compared to other alkenes derivatives.
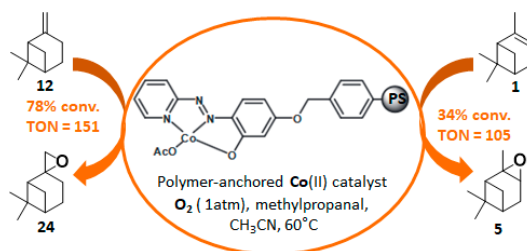
Figure 7. Aerobic oxidation of pinene isomers using a polymer-anchored Co(II) catalyst (adapted from reference [41]).

Titanium catalysts. The same team developed a series of Ti-MCM-41 catalysts, in which the metal species were incorporated by post-synthesis methods, such as wetness (WN1) and wet (W1) impregnation of the MCM-41 mesoporous materials [42]. Compared with catalysts obtained through a hydrothermal (HT) approach, the solids present a well-ordered hexagonal arrangement, with three types of titanium sites. The performances of these catalysts were evaluated in the oxidation of limonene **2** with H_2O_2 in acetonitrile (Table 9).

Table 9. Oxidation of limonene with titanium-MCM-41 catalysts [a] (adapted from reference [42]).

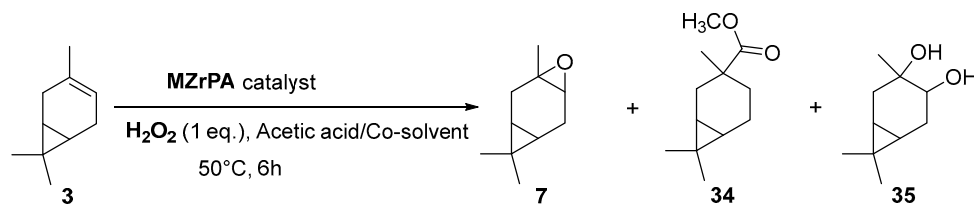| Entry	Catalyst	% TiO₂ (*w/w*)	χ_L [b] (% max)	TOF [c] (h⁻¹)	Efficiency H₂O₂ [d]	Product Selectivity [e] (%)		
						6 + 30 [f]	9 + 17	Others [g]
1	WN1	1.8	50	3.4	68	46	34	20
2	W1	7.3	48	0.9	59	50	31	19
3	HT	1.8	52	4.5	65	58	22	20

[a] Reaction conditions: Catalyst (50 mg), limonene (4.32 mmol), H_2O_2 (0.25 eq.), CH_3CN, 70 °C, 7 h. [b] Limonene conversion as percentage of the maximum possible conversion. [c] TurnOver Frequency to epoxides. [d] Percentage of H_2O_2 consumed to produce oxygenated products. [e] Expressed as a percentage of the total formed products. [f] 1,2- and 1,8-epoxylimonene. [g] Diepoxide and glycol.

The structural differences did not change significantly the catalytic activities, with about 50% of conversion for each material. Nevertheless, a slight decrease in the selectivity in epoxide is observed with Ti-MCM-41 catalysts prepared by the post-synthetic approach (Entries 1–2), in favor of the allylic oxygenated products (carvone **9** and carveol **17**). Despite these quite lower catalytic performances, the authors claimed an easier and reproducible post-synthetic method for the catalyst's recycling.

2.2.4. Miscellaneous Metals

In this part, some unconventional metals, such as zirconium, niobium, and praesodynium, are described, generally with hydrogen peroxide or air as oxidant.

Zirconium catalysts. In 2009, Rocha et al. compared the catalytic performances of various zirconium-based tetravalent phosphates and phosphonates in the oxidation of (+)-3-carene **3** using hydrogen peroxide [43]. Metal(IV) phosphates and phosphonates are particularly pertinent owing to their low cost, easy synthesis, and extreme resistance to high temperatures. First, the authors showed that the oxidation reaction occurred in glacial acetic acid, alone or with co-solvents (dichloromethane or acetonitrile), but not in organic solvents alone. This solvent effect presumes that peracetic acid formed during the catalytic process is the effective oxidant. Three major oxidation products were formed: α-3,4-epoxycarane **7**, 3β-acetoxycaran-4α-ol **34** from the acidic cleavage of epoxide, and carane-3β,4α-diol **35** after acid hydrolysis. Considering the results in Table 10, it seems that the judicious combination of solvent or solvent mixtures, with a metal(IV) phosphates or phosphonates possessing basic properties (NaZrPA or KZrPA), leads to promising selectivities in epoxide.
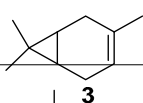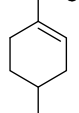
Table 10. Metal phosphates or phosphonates-catalyzed oxidation of 3-carane [a] (adapted from reference [43]).

Entry	Catalyst	Solvent	Conv. (%)	Selectivity (%)		
				7	34	35
1	NaZrPA	AcOH	31.6	61.4	38.3	-
2	KZrPA	AcOH	36.1	58.2	33.5	-
3	NaZrPA	CH$_2$Cl$_2$/AcOH (1/1)	57.5	58.3	20.7	7.9
4	KZrPA	CH$_2$Cl$_2$/AcOH (1/1)	50.4	48.3	21.5	16.1
5	ScZrPA	CH$_2$Cl$_2$/CH$_3$CN/AcOH (1/1/0.2)	20.7	100	-	-
6	ZrPPA	CH$_2$Cl$_2$/CH$_3$CN/AcOH (1/1/0.2)	14.6	100	-	-

[a] Reaction conditions: Catalyst (58 mg), 3-carene (2.2 mmol), H$_2$O$_2$ (1 eq., 35% w/w), 2 mL solvent, 50 °C, 6 h, PA = Phosphate, PPA = Phosphonate.

Niobium catalysts. Some studies showed that niobium containing silicates are active catalysts for the epoxidation of olefins with hydrogen peroxide, being more resistant to hydrolysis and metal leaching [44]. Based on these promising results, Kholdeeva and coworkers prepared mesoporous niobium-silicates by an evaporation-induced self-assembly (EISA) method in order to control the state of metal centers according to the niobium precursor [45]. On one hand, the use of niobium(V) ethoxide modified with acetylacetone leads to the formation of oligomeric metal species well-dispersed within the silica matrix (Catalyst A). On the other hand, ammonium niobate(V) oxalate hydrate in combination with acetylacetonate affords catalytic materials with isolated niobium species (Catalyst B). Both catalysts were efficiently used in the epoxidation of two terpenic olefins—limonene **2** and 3-carene **3**—using hydrogen peroxide as oxidant (Table 11).

Table 11. Oxidation of 3-carene and limonene using mesoporous niobium-silicates [a] (adapted from reference [45]).

Entry	Substrate	Catalyst	Solvent	Time [b] (h)	Conv. [c] (%)	Epoxide Selectivity [d] (%)	*Exo/Endo* Ratio [e]
1		A	CH$_3$CN	2	20	>99	-
2		B	CH$_3$CN	1	26	>99	-
4		A	CH$_3$CN	2	29	73	n.d [f]
5		B	CH$_3$CN	2	28	71	2.7
6		B	MeOH	2	12	90	0.5
7		B	Dimethyl carbonate	2	10	43	2

[a] Reaction conditions: Catalyst A (0.003 mmol Nb) or B (0.005 mmol Nb), substrate (0.1 mmol), 50% H$_2$O$_2$ (1 eq.), solvent (1 mL), 50 °C. [b] Optimal reaction time for maximum selectivity and conversion. [c] Determined by GC analyses. [d] Other products: carveol, carvone, and limonene diepoxide. [e] Ratio of exocylic epoxide (7,8-limonene epoxide) to endocyclic epoxide (1,2-limonene epoxide). [f] Non determined.

For 3-carene **3**, a complete selectivity toward epoxide was obtained with an acceptable olefin conversion of about 30% (Entries 1–2). However, this value tends to drop at higher conversions, owing to the formation of co-products resulting from rearrangement, ring-opening, and suroxidation processes. Concerning limonene **2**, a drastic influence of the solvent on the exo- to endocyclic ratio was observed (Entries 5–7). While 1,2-limonene epoxide was predominantly formed in methanol,

7,8-limonene epoxide was obtained in acetonitrile (Entry 5 vs. 6). These differences of selectivity suggest that different reaction mechanisms could be involved. Finally, these quite robust catalysts could be easily recycled due to no metal leaching observed.

Praesodynium catalysts. Interestingly, Jang and coworkers developed praesodynium-containing AlPO-5 material through a hydrothermal method in fluoride medium using triethylamine as template [46]. This bifunctional catalyst, possessing both redox and mild acid sites, allows the production of campholenic aldehyde **26**, an industrial relevant synthon for the production of santalol (sandalwood fragrance) [47], from α-pinene **1** via the epoxide **5** as intermediate. This compound was selectively isomerized into campholenic acid due to the Lewis acid sites in the framework of the material. It is noticeable that the catalyst with a lower (Al+P)/Pr ratio leads to higher catalytic performances in terms of activity, product selectivity, and reusability over five runs, as presented in Scheme 9.
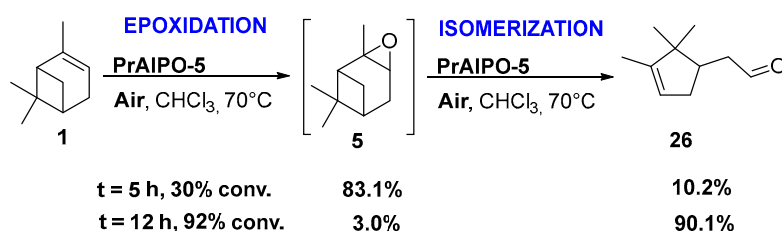
Scheme 9. Epoxidation-isomerization process, catalyzed by PrAlPO-5 material (with (Al+P)/Pr ratio of 75) for the production of campholenic aldehyde (adapted from reference [46]). Product selectivities are given for α-pinene oxide **5** and campholenic aldehyde **26**.

2.3. Catalysts Comparison and Conclusions

Catalytic epoxidation reactions of terpenic olefins constitute valuable synthetic transformations for the production of epoxides and diols as relevant intermediates for various chemical industries. As illustrated alongside this first part, the control of the selectivity in epoxidation remains quite challenging, with the competitive formation of allylic oxidation products, as well as rearrangement, isomerization, or suroxidation. Moreover, in some cases, the formation of epoxides seems to be substrate-dependent, and it therefore becomes difficult to predict and rationalize the result of the reaction. The Figure 8 presents a comparison of various catalysts and oxidants used in the epoxidation of α-pinene **1**, one of the most studied terpenic olefins.
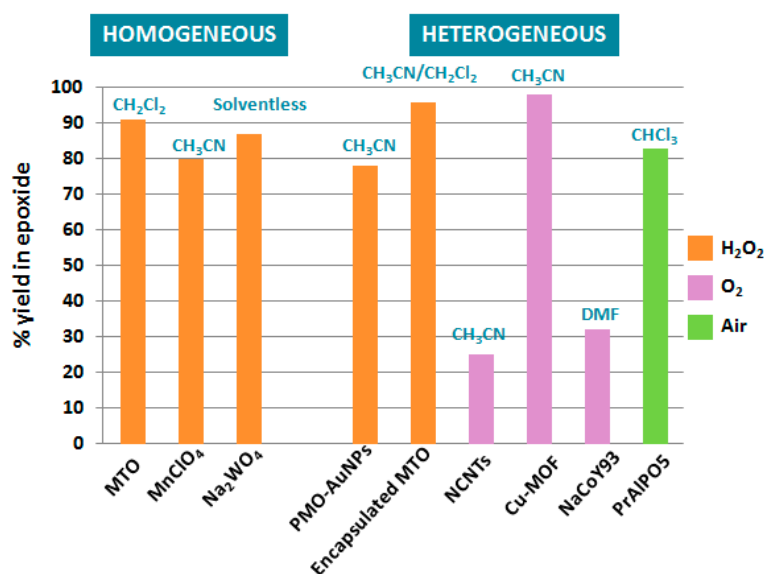
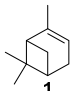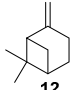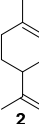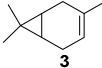**Figure 8.** Overview of catalytic systems for epoxidation of α-pinene.

From this comparative study, either homogeneous or heterogeneous catalysts, based on semi-noble rhenium catalysts (MTO) or first row transition metals, such as manganese or copper species, are relevant candidates to transform α-pinene **1** into the corresponding epoxide, using either hydrogen peroxide or dioxygen as green oxidants. Although homogeneous and heterogeneous rhenium catalysts affords quite efficient catalytic performances with various terpenes, these processes use toxic additives, as well as organic solvents, which are considered as problematic and hazardous according to some solvent selection guides [48]. In that context, Nardello-Rataj and coworkers investigated 18 eco-friendly solvents for the epoxidation of various olefins, catalysed by amphiphilic dodecyltrimethyl ammonium polyoxometalate nanoparticles $[C_{12}]_3[PW_{12}O_{40}]$ [49]. Among these solvents, cyclopentylmethylether (CPME) and 2-methyltetrahydrofuran (2-Me-THF) were found more efficient and extended to several terpenic olefins through a sequential addition of hydrogen peroxide to achieve better selectivities (Table 12). Higher selectivities and catalytic activities were achieved with limonene **2** and 3-carene **3**, as usually observed, compared to pinene isomers **1** and **12**, which are more prone to oligomerizations and rearrangements [50].

Table 12. Epoxidation of terpenes, catalyzed by $[C12]_3[PW_{12}O_{40}]$ nanoparticles in CPME or 2-Me-THF [a] (adapted from reference [49]).

Entry	Substrate	Solvent	Selectivity [b] (%)	TOF_0 (h^{-1})
1 [c]	**1**	CPME	49	23.5
		2-Me-THF	51	30.0
2 [c]	**12**	CPME	43	35.4
		2-Me-THF	45	32.3
3 [d]	**2**	CPME	65 [e]	53.0
		2-Me-THF	73 [e]	61.0
4 [d]	**3**	CPME	68	56.2
		2-Me-THF	72	49.7

[a] Reaction conditions: Catalyst (15 μmol), substrate (1.5 mmol), H_2O_2, Solvent (3 mL), 65 °C. [b] Determined by GC. [c] 0.5×4 equiv. H_2O_2, 4 h. [d] 0.5×3 equiv. H_2O_2, 3 h. [e] Limonene 1,2-epoxide.

3. Allylic Oxidation of Terpenic Olefins

Oxidation of allylic methylene groups into their conjugated carbonyl derivatives also remains a relevant value-creating Csp^3-H functionalization approach to produce value-added products [51]. The allylic oxidation of terpenic olefins was previously performed using stoichiometric amounts of toxic chromium- or selenium-based reagents without fulfilling the criteria of eco-responsible chemistry [8]. Therefore, various greener methods have been developed to transform these renewables into allylic oxidation products such as α,β-unsaturated ketones. An overview of the last 10 years' literature is presented hereafter.
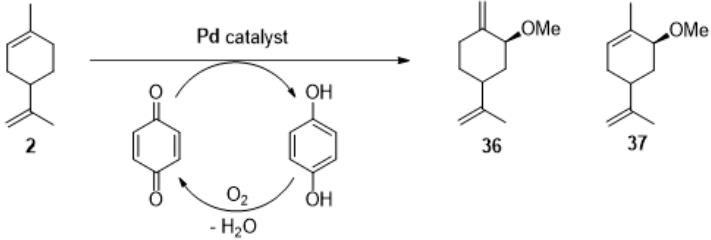
3.1. Using Homogeneous Complexes Based on Noble Metals

First, molecular complexes, exclusively based on noble metals such as palladium or rhodium, were used for this transformation.

Palladium catalysts. Palladium complexes could be used as efficient catalytic systems, combined with reversible co-oxidants for the re-oxidation of the zerovalent metal species such as the

CuCl$_2$ (Wacker-type catalyst). In that context, Gusevskaya and coworkers developed a selective palladium-catalyzed oxidation process for limonene **2** in the presence of benzoquinone as redox agent and of various alcohols as nucleophiles to access the corresponding allylic ethers [52]. The results obtained with methanol, gathered in Table 13, could be extended to other alcohols (ethanol, propan-2-ol, etc.).

Table 13. Oxidation of limonene **2** catalyzed by palladium complexes in methanol [a] (adapted from reference [52]).
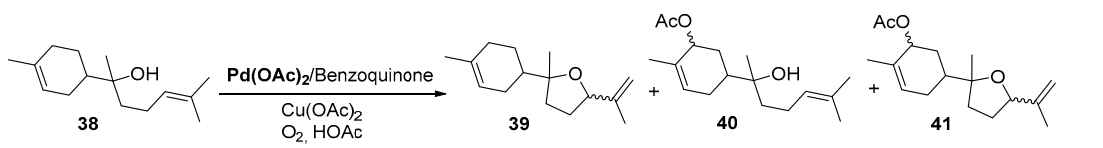

Entry	[Pd]	PTSA (M)	T (°C)	Time (h)	Conv. [b] (%)	% 36 [b]	% 37 [b]
1	Pd(OAc)$_2$	0.02	25	2	80	98	-
2	Pd(OAc)$_2$	0.04	25	2	94	97	-
3	Pd(OAc)$_2$	0.04	25	3	98	97	-
4	Na$_2$PdCl$_4$	0.02	80	4	99	6	55
5	Pd(acac)$_2$	0.06	25	1	28	95	-
6	Pd(acac)$_2$	0.06	25	20	98	95	-

[a] General conditions: [Limonene] = 0.2 M, [Pd] = 0.01 M, [Benzoquinone] = 0.4 M, PTSA = *p*-toluenesulfonic acid.
[b] Determined by Gas Chromatography.

First, *p*-toluenesulfonic acid (PTSA) is known to promote a kinetic effect on the reaction rate and a stabilizing influence on the catalyst. Moreover, an increase in PTSA concentration (Entries 1,2) leads to higher reaction rates, without modifying the reaction selectivity towards the ether **36** containing two exocyclic double bonds. In the same manner, the palladium precursor seems also to have an influence. While the Pd(acac)$_2$ precursor gives similar results in terms of selectivity in **36** with a lower reaction rate (Table 13, Entries 5–6), the selectivity switches towards the ether **37** with Na$_2$PdCl$_4$ as catalyst (Table 13, Entry 4). In 2014, quite a similar catalyst, based on Pd(OAc)$_2$ combined with benzoquinone, was used for the aerobic oxidation of α-bisabolol **38**, a bio-renewable present in various essential oils [53]. This process leads to the formation of three main products: the product **39** via the oxidation of the exocyclic encumbered double bond, combined with the hydroxyl-assisted formation of the tetrahydrofuran ring, and the allylic acetates **40** and **41** by allylic oxidation of the endocyclic double bond, or both olefinic bonds. The reaction conditions were optimized to find adequate conditions to regenerate benzoquinone (BQ) and use this oxidant in catalytic amounts. Some of the results, resulting from this screening study, are gathered in Table 14. First, as a comparison experiment (Table 14, Entry 1), the reaction with a stoichiometric amount of benzoquinone proceeded with a 58% conversion in 5 h and a 88% selectivity in **39** and **40**. The authors showed that copper acetate could be used as a catalytic transfer mediator, thus allowing the efficient regeneration of benzoquinone during the catalytic cycle (Table 14, Entries 2–6) and its sub-stoichiometric use (up to 0.25 equiv.). Moreover, benzoquinone seems to be crucial toward the selectivity all over the reaction (Table 14, Entries 4–6) acting as a ligand of palladium system.

Table 14. Palladium-catalyzed oxidation of α-bisabolol **38** with molecular oxygen in the presence of benzoquinone and copper acetate [a] (adapted from reference [53]).

Entry	[BQ] (mol·L^{-1})	[Cu(OAc)$_2$] (mol·L^{-1})	T (°C)	Time (h)	Conv. (%) [b]	Selectivity [b] (%)			
						39	40	41	Total
1	0.2	None	60	5	58	46	32	12	90
2	0.05	0.05	80	12	90	27	21	42	90
3	0.05	0.025	80	12	85	30	23	27	80
4	0.02	0.025	80	1	25	45	28	2	75
5	0.02	0.025	80	4	50	39	28	22	78
6	0.02	0.025	80	8	70	32	24	18	74
7 [c]	0.02	None	80	7	80	38	24	18	80

[a] General conditions: [α-bisabolol] = 0.2 M, [Pd] = 0.01 M, Benzoquinone, HOAc, gas-phase O$_2$ (1 atm). [b] Determined by Gas Chromatography analyses and calculated on the consumed substrate. [c] 10 atm of O$_2$.

In 2009, da Silva et al. reported a complex PdCl$_2$/H$_2$O$_2$/CH$_3$CN system, which transformed camphene into the corresponding epoxide (*vide supra*) [14]. In contrast, the same catalyst used with β-pinene **12** afforded allylic oxidation products, mainly pinocarveol **13** (57%) and pinocarvone **14** (24%), alongside epoxy-β-pinene **24** (19%), with a conversion up to 58% in 8 h (Scheme 10).
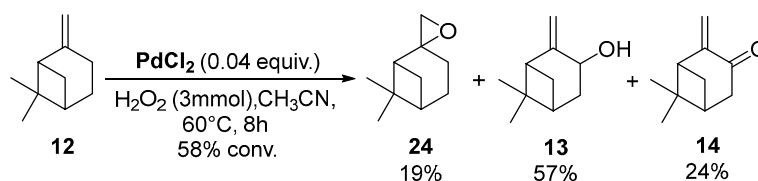
Scheme 10. PdCl$_2$-catalyzed oxidation of β-pinene **12** by H$_2$O$_2$ (adapted from reference [14]).

Nevertheless, under these conditions, α-pinene **1** provides a complex mixture of products, without oxidation compounds, probably due to the steric hindrance of the methyl groups. On the contrary, the oxidation of 3-carene **3** gave various allylic oxidation products (mono- and di-ketones, allylic alcohols and little epoxy-derivatives) with low degree of selectivity.
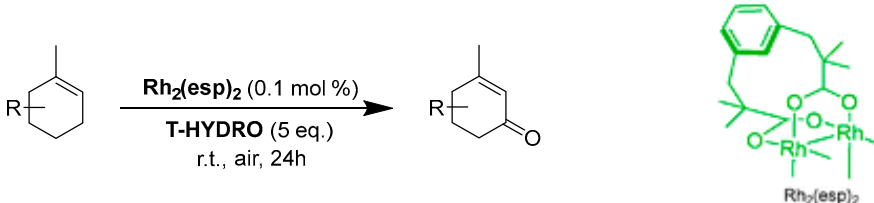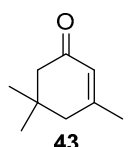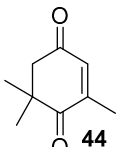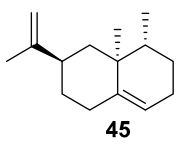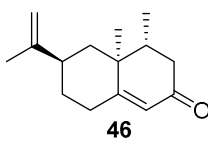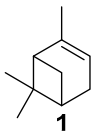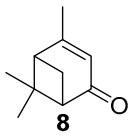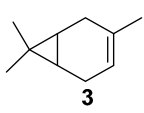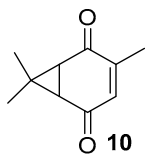
Rhodium catalysts. In 2009, Doyle *and coworkers* reported the use of dirhodium(II) caprolactamate (Rh$_2$(cap)$_4$) (E$_{1/2}$ = 11 mV [54]) as a catalyst for the oxidation of (*R*)-(+)-limonene **2** [55], with a safer and cheaper 70% *t*-BHP in water (T-HYDRO) as an oxidant (Scheme 11). After 20 h, the reaction afforded racemic carvone **9** as major product with a 44% isolated yield, resulting from the racemic free radical obtained by H-abstraction at the 6-position of the substrate. Isopiperitinone **42**, arising from oxidation at the 3-position, was also observed as a minor product, probably owing to steric factors.
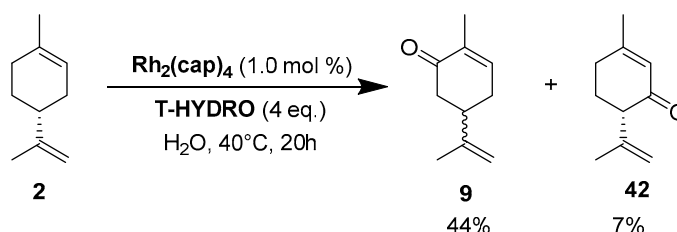
Scheme 11. Rh$_2$(cap)$_4$-catalyzed allylic oxidation of limonene **2** (adapted from reference [55]).

Recently, the chelating Du Bois' catalyst Rh$_2$(esp)$_2$ (esp= α,α,α′,α′-tetramethyl-1,3-benzene dipropionate), possessing a higher oxidation potential (E$_{1/2}$ = 1130 mV [56]) proved to efficiently

catalyze the solvent-free allylic oxidation of some targeted olefins, using large excess of T-HYDRO (5 equiv.), at ambient temperature (Table 15) [57]. First, the $Rh_2(esp)_2$ catalyst was more efficient than $Rh_2(cap)_4$ complex for oxidation of isophorone **43**, a structural model of terpenic derivatives, with a 91% conversion in 24 h. Moreover, the catalyst was easily separated by chromatographic purification and reused. After optimization on isophorone, the process was successfully extended to some targeted terpenic olefins (Entries 2–4), leading to the corresponding α,β-unsaturated ketones with promising isolated yields, ranging from 43 to 71%.

Table 15. Allylic oxidation of olefins by $Rh_2(esp)_2$/T-HYDRO under optimized reaction conditions [a] (adapted from reference [57]).

Entry	Substrate	Product	Yield [b] (%)
1	**43**	**44**	78
2	**45**	**46**	71
3 [c]	**1**	**8**	43
4 [c]	**3**	**10**	60

[a] General conditions: Olefin (4 mmol), $Rh_2(esp)_2$ (0.1 mol%), T-HYDRO (20 mmol), r.t. [b] Isolated yield. [c] $Rh_2(esp)_2$ (1 mol%) and 1 mL H_2O.

3.2. Using Heterogeneous Catalysts

Chromium reagents are widely known in stoichiometric or catalytic oxidations. However, with regard to environmental considerations, the most relevant approach consists in the catalytic use of chromium species deposited on heterogeneous supports [58]. In the first paragraph, some of the most pertinent chromium-based systems will be referenced. Then, novel catalysts composed of noble and first row transition metals will be described.

3.2.1. Chromium-Based Catalysts

Various chromium-containing solid materials were developed and evaluated in the oxidation of α-pinene **1**, using either *tert*-butylhydroperoxide (*t*-BHP) or molecular oxygen. The main detected

products are verbenone **8**, verbenol **32**, epoxide **5**, and α-pinenehydroperoxide **33**. Table 16 gathered some of the most pertinent chromium heterogeneous catalysts.
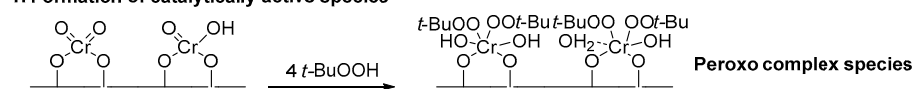
Chromium catalysts, deposited either on MIL-101 framework [59] or SBA-15 support [60], are active and selective toward α,β-unsaturated ketones with *t*-BHP and reusable with no leaching of the metal from the inorganic matrix. Mechanistically, the reaction mainly occurs via a heterolytic pathway and proceeds via a radical-chain mechanism (Scheme 12) [60]. Promising catalytic performances are also observed with chromium-containing mesoporous materials (MCM-41 or MIL-101) in aerobic conditions [12,61]. This catalytic system was extended to β-pinene **12**, mainly affording the allylic mono-oxygenated products [12]. Interestingly, Kholdeeva et al. [61,62] compared the potential of both chromium- and iron-containing mesoporous metal-organic framework (MIL-101) in the solventless oxidation of some terpenes, such as α- and β-pinenes **1** and **12**, respectively, and limonene **2**. The product distribution seems to be dependent on the nature of the metal (Table 17). Various products were identified, probably due to the partial isomerization of the substrate and the resulting products. On one hand, chromium-based catalysts give the α,β-unsaturated ketone, through dehydration of the hydroperoxide, followed by the subsequent oxidation of the corresponding alcohol into ketone. On the other hand, iron catalyst affords the alcohol, resulting from the metal-centered oxidation. In the case of limonene **2**, the epoxide **6** was also observed (Table 17, Entry 3a-b). The catalysts could be recycled at least four times with no loss of the catalytic properties. Moreover, the authors evaluated the effect of the support in the oxidation of pinene isomers (Table 17, Entries 1c-d and 2c-d) using an MIL-101 support with cages presenting diameters of 34 and 29 Å as well as an MIL-100 structure with smaller cages (24 and 27 Å) [63]. No significant influence of the material was noticed on the catalytic performances.

Table 16. Chromium-containing solid materials for allylic oxidation of α-pinene **1**.

Entry	Catalyst	Cr (mmol)	Oxidant	Solvent	T (°C)	Conv. (%)	Enone Selectivity (%)	Ref.
1 [a]	Cr-SBA15(8)	n.d. [c]	*t*-BHP	Chlorobenzene	85	91.5	88.2	[61]
2 [b]	Cr-SBA15(8)	n.d. [c]	*t*-BHP	Chlorobenzene	85	85.2	80.1	[61]
3 [a]	Cr-MIL-101	0.006	*t*-BHP	Benzene	50	87	89	[62]
4 [b]	Cr-MIL-101	0.006	*t*-BHP	Benzene	50	90	87	[62]
5	Cr-MCM41	0.02	O_2 (1 bar)	Solventless	60	40	26	[12]
6	Cr-SiO$_2$	0.02	O_2 (1 bar)	Solventless	60	45	16	[12]
7	Cr-MIL-101	0.1	O_2 (10 bar)	Solventless	60	26	39	[63]

[a] Cr-SBA15(8) prepared with a pH-adjusting hydrothermal method according to a n_{Si}/n_{Cr} = 8. [b] Reusable Cr-containing solid catalyst was used in a second run. [c] Non determined.

Scheme 12. Proposed mechanism for the oxidation of α-pinene over Cr-SBA-15 (adapted from reference [60]).

Table 17. Iron- vs. chromium-MIL catalysts—a comparison in the oxidation of various terpenic olefins [a] (adapted from reference [61–63]).

Entry	Metal	Support	T (°C)	Conv. (%)	Product Selectivity (%)			
					13	**16**	**14**	**15**
1a	Cr	MIL-101	60	22	32	23	27	
1b	Fe	MIL-101	40	13	57	-	-	
1c	Cr	MIL-100	60	18	20	2	33	
1d	Fe	MIL-100	40	12	64	-	10	
					32	**8**	**47**	
2a	Cr	MIL-101	60	26	31	39	8	
2b	Fe	MIL-101	40	12	33	-	33	
2c	Cr	MIL-100	60	20	15	30	9	
2d	Fe	MIL-100	40	9	32	-	15	
					17	**9**	**6**	
3a	Cr	MIL-101	60	13	2	21	38	
3b	Fe	MIL-101	40	6	16	12	35	

(Olefin structures shown: **12**, **1**, **2**; products **13**, **16**, **14**, **15**, **32**, **8**, **47**, **17**, **9**, **6**.)

[a] General conditions: 12–26 mg catalyst (0.05–0.1 mmol Fe or Cr), 10 mmol olefin, 1 bar O_2, *t*-BHP (0.02 mmol), 16 h.

3.2.2. Noble Metals

Ruthenium and gold catalysts. Godhani et al. prepared zeolite-Y encaged ruthenium(III) and iron(III) complexes, modified with a Schiff Base (SB) ligand (2,2′-((1E,1′E)-((azanediylbis(ethane-2,1-diyl))bis(azanylylidene))bis(methanylyliden)diphenol) [64] and compared their catalytic results in the oxidation of limonene **2** with H_2O_2 (Figure 9). First, the homogeneous Ru-SB catalyst was more efficient than its heterogeneous Ru-SB-Y analog. However, the zeolite-Y encaged Ru(III) complex presents a higher TurnOver Frequency (2273 h^{-1} vs. 50.8 h^{-1} for Ru-SB) and is more easily recycled. Both molecular and heterogeneous catalysts were highly selective in allylic products (80–90%), with carvone **9** as major product, and more active than the metal exchanged zeolite-Y materials.

	NaY	MY		M-SB-Y		
	Sodium zeolite-Y	Metal exchanged zeolite-Y		Zeolite-Y encapsulated complexes		
		FeY	RuY	Fe-SB-Y	Ru-SB-Y	Ru-SB[c]
Limonene conversion (%)	4.6	17.5	12.6	78.9	81.6	96.6
H_2O_2 Efficiency (%)	28	23	15.2	82.2	81.6	97.6
Carveol (%)	47.8	31	27.4	19.1	11.2	16.5
Carvone (%)	14.3	28.6	34.3	61.2	78.4	70.3
Epoxidation products[b] (%)	37.9	40.4	38.3	19.7	10.4	13.2

[a] Reaction conditions: Catalyst (12.5 mg), limonene (25 mmol), 30%-H_2O_2 (25 mmol), CH_3CN (6 mL), 80 °C, 18 h. [b] Epoxidation products = Limonene oxide, limonene dioxide, limonene glycol. [c] Ru(III) complexes prepared from $RuCl_3.3H_2O$ and Schiff Base.

Figure 9. Allylic oxidation of limonene with zeolite-Y encaged Ru(III) and Fe(III) complexes. Comparison of various catalytic systems (adapted from reference [64]).

The Ru-SB-Y material was applied to α-pinene **1**, affording the allylic products (verbenone **8**, verbenol **32** and myrtenol **16**) with a 87% selectivity and a TOF up to 2023 h^{-1} (Figure 10). Surprisingly, the addition of sulfuric acid in the reaction media favored the epoxidation products (pinene oxide **5** and campholenal 26) without their opening, with a complete conversion and a 70% selectivity.
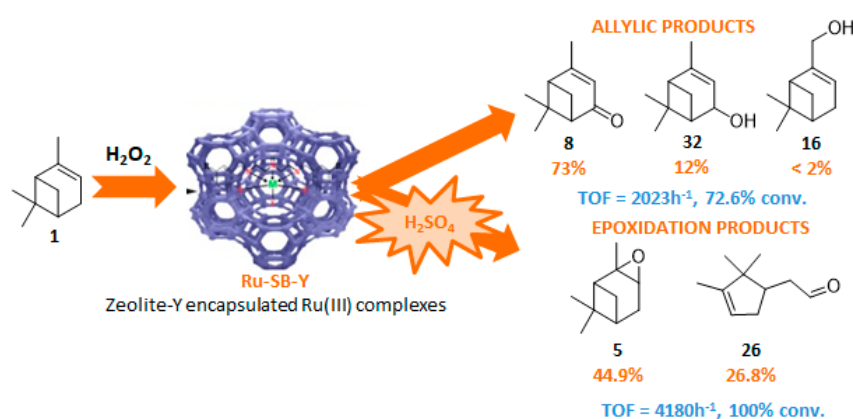
Figure 10. Oxidation of α-pinene with zeolite-Y encaged Ru(III) complex. Influence of H_2SO_4 (adapted from reference [64]).

In 2011, Mikkola and coworkers studied the catalytic performances of TiO_2-supported bimetallic gold-metal (with metal = Cu, Co, Ru) nanoparticles, obtained by a deposition–precipitation method [65]. Transmission Electron Microscopy images showed finely distributed particles on the support in the size range of 3–4 nm and 4–6 nm, respectively for the bi- and mono-metallic catalysts. XPS (X-ray photoelectron spectrometry) studies validate the formation of metallic Au^0 particles under the synthesis conditions (300 °C), while other metals (cobalt, copper, ruthenium) are in oxide forms. Various reaction parameters (reaction time, temperature, solvent) were studied to achieve optimal conversion of α-pinene **1** in verbenone **8**. Under optimized conditions, a comparison of the various catalysts is resumed in Table 18. The bimetallic $AuCu/TiO_2$ (1/1) was more active and selective in ketone **8** (Entry 2). The catalytic activities over the various systems decreased in the following order: $AuCu/TiO_2$ > $AuCo/TiO_2$ > Cu/TiO_2 > Au/TiO_2 > $AuRu/TiO_2$. Finally, the $AuCu/TiO_2$ catalyst was easily recycled, with a conversion up to 94% for three successive runs.

Table 18. Oxidation of α-pinene. Comparison of various gold containing mono- or bi-metallic nanoparticles supported on TiO_2 [a] (adapted from reference [65]).

Entry	Catalyst	Conversion (%) [b]	Selectivity (%) [b]		
			Verbenone 8	Verbenol 32	Epoxide 5
1	-	62	21.6	12.8	19.2
2	$AuCu/TiO_2$	97	47.9	12.1	6.5
3	$AuCo/TiO_2$	88	28.2	13.2	6.3
4	$AuRu/TiO_2$	73	32.1	22.1	5.7
5	Au/TiO_2	78	24.6	17.5	4.6
6	Cu/TiO_2	80	22.8	8.8	8.5

[a] Reaction conditions: Catalyst (100 mg), α-pinene (5 mmol), *t*-BHP (5 mmol), CH_3CN (15 mL), 70 °C. [b] Determined by Gas Chromatography.

3.2.3. First Row Transition Metals

Iron catalysts. Iron—a cheap, non-toxic, and earth-abundant metal—was deposited on various supports (activated carbon, silica, or montmorillonite). First, activated carbon EuroPh supported-iron catalysts, with various metal contents were evaluated in the oxidation of limonene **2** (Table 19) with hydrogen peroxide (H_2O_2) or *tert*-butylhydroperoxide (*t*-BHP) [66].

Table 19. FeEuroPh-catalyzed allylic oxidation of limonene **2**: H_2O_2 vs. *t*-BHP [a] (adapted from reference [66]).

Entry	Fe Content (%)	Oxidant	Selectivity [b] (%)				
			9 (%)	17 (%)	48 (%)	6 (%)	31 (%)
1	0.68	H_2O_2	28	-	50	-	22
2	1.32	H_2O_2	22	-	44	-	34
3	2.64	H_2O_2	-	-	37	-	63
4	0.68	*t*-BHP	24	-	76	-	-
5	1.32	*t*-BHP	18	10	72	-	-
6	2.64	*t*-BHP	-	-	73	27	-

[a] Reaction conditions: Catalyst (2.45% wt.), (*R*)-limonene (1.6% wt.), limonene/oxidant = $\frac{1}{2}$, Methanol, 70 °C. [b] Determined by GC analyses.

Whatever the oxidant is, the main product is the perillyl alcohol **48** obtained by allylic oxidation at position 7. At low iron loading, carvone **9** was also observed with selectivities around 20–30% (Entries 1,2 and 4,5). However, epoxidation of the unsaturated bond at the 1,2 position of limonene, followed by hydration to afford the corresponding diol **31**, also occurs with hydrogen peroxide. At higher metal loading, 1,2-epoxylimonene **6** was also detected with *t*-BHP (Entry 6). In 2016, Gonzalez et al. immobilized an iron hexadecachlorinated phthalocyanine on a modified silica ($FePcCl_{16}$-NH_2-SiO_2) and studied the kinetics of the oxidation of α-pinene **1**, using *tert*-butylhydroperoxide in acetone (Figure 11) [67]. After 23 h, a conversion up to 83.7% was achieved, with 23% of selectivity in verbenone **8**. The catalyst could be efficiently reused over 7 runs, with no significant loss of activity. Kinetic studies suggested that the oxidation over this supported catalyst was not purely heterogeneous but also homogeneous, owing to the involvement of radical species in the bulk phase.
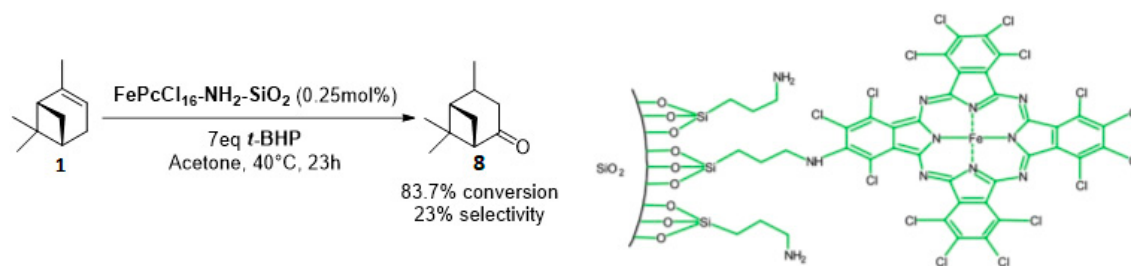
Figure 11. FePcCl$_{16}$-NH$_2$-SiO$_2$-catalyzed oxidation of α-pinene (adapted from reference [67]).

In 2006, mechanochemically activated iron-pillared montmorillonite materials (Fe-PILC/MA) were prepared and investigated in the same reaction, but in dichloromethane (Figure 12) [68]. These materials are characterized by a "house cards" structure of Fe$_2$O$_3$-pillars and meso- and macropores. They were compared to iron-supported on sodium-montmorillonite (Fe-PILC), mainly formed of Fe$_2$O$_3$-pillars and micropores. According to the structural features of the materials, isomerization (such as limonene **2** or *p*-cymene **49**) or oxidation products were obtained. Thus, the Fe- PILC material mainly leads with high conversion to the α-isomerization product, limonene **2**, alongside *p*-cymene **49** and some fragmentation products. On the contrary, the mechanochemically activated material affords lower conversion, but high selectivity in allylic oxidation products **8** and **32** (67.5%), with α-campholene aldehyde **26** (7%) formed by rearrangement of epoxypinane on the acidic sites of the support. Finally, an increase in the oxidant amount allows total conversion, with an 84% ketone yield.
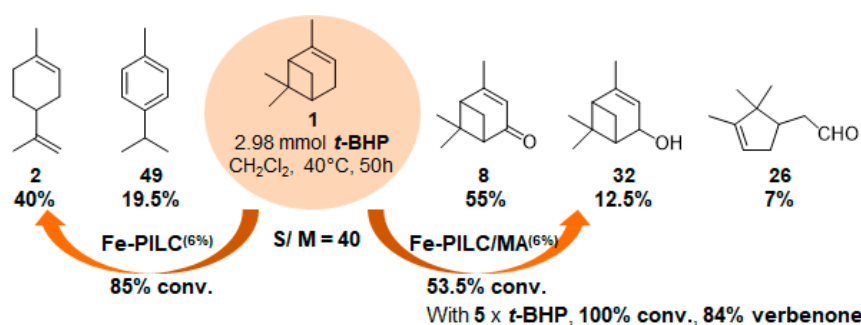
Figure 12. Influence of the type of Fe-pillared montmorillonite on α-pinene oxidation (Fe-PILC: Fe-pillared montmorillonite, Fe-PILC/MA: mechanochemically activated Fe-pillared montmorillonite) (adapted from reference [67]).

Manganese oxide catalysts. Activated MnO$_2$, combined with *tert*-butylhydroperoxide, proved to be an efficient system for the oxidation of allylic methylene groups of limonene **2** or valencene **45**, into the corresponding α,β-unsaturated ketones with 22% (carvone **9**) and 63% (nootkatone **46**) yields, respectively (Figure 13) [69]. The oxidation process proceeds in two sequential steps: first, at low temperature (−30 to −10 °C), the oxide species catalyzes the oxidation of the methylene group; secondly, at higher temperatures, it decomposes the unreacted *t*-BHP and oxidizes the formed allylic alcohol.

In 2013, Panda and coworkers developed a new method for the synthesis of porous hierarchically ordered lotus-shaped MnO$_2$ nanomaterial, obtained by a chelate-mediated growth of MnCO$_3$ using citric acid as a chelating agent, followed by calcination [70]. This material was compared to other MnO$_2$ nanospecies, possessing different morphologies (rods, spheres, or aggregates) prepared from other chelating agents (tartaric acid, oleic acid, or ethylenediaminetetraacetic acid known as EDTA), as well as to bulk manganese. Among the tested catalysts, the lotus-shaped form showed excellent catalytic results in the solventless oxidation of α-pinene **1** using dioxygen as oxidant (Table 20), with a 82% yield in verbenone **8**.
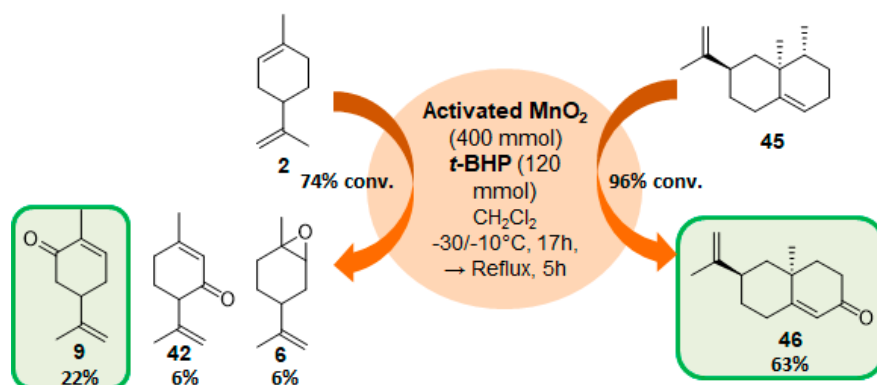
Figure 13. Combined use of MnO_2 and *t*-BHP for the oxidation of some terpenes (adapted from reference [69]).

Table 20. Allylic oxidation of α-pinene. Comparison of various shaped MnO_2 catalysts [a] (adapted from reference [70]).

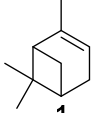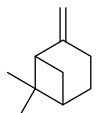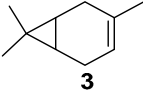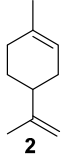| Entry	Morphology	$d_{(XRD)}$ [b] (nm)	S_{BET} [c] (m^2 g^{-1})	Conversion [d] (%)	Selectivty [e] (%)
1	Lotus	7	145	94	87
2	Rods	7.3	92	80	70
3	Spheres	7.5	109	86	79
4	Agglomerates	6.5	56.9	81	87.5
5	Bulk	-	3	64	59

[a] Reaction conditions: Catalyst (55 mg), substrate (25.2 mmol), O_2 (1 bar), 75 °C [b] Crystallite size determined from XRD line broadening. [c] BET surface area. [d] Conversion of α-pinene, determined by GC analyses. [e] Selectivity in verbenone determined by GC analysis.

Cobalt catalysts. At the end of 1990s, molecular cobalt complexes, such as $Co(NO_3)_2$ or $Co(4\text{-MeC}_5H_3N)_2Br_2$, proved to be active for the oxidation of α-pinene **1** with promising selectivities [71–73]. Their supported analogs have also been widely studied. For instance, Gusevskaya et al. used inexpensive cobalt- and manganese-substituted ferrites as heterogeneous materials in the solventless and mild oxidation of model monoterpenes (Table 21), with molecular oxygen (1 bar O_2) [74]. From characterization studies, the substitution of iron by cobalt or manganese species in the ferrite structure preferentially occurred at octahedral positions. First, cobalt-containing ferrites seem to be slightly more active with higher TONs, compared to the manganese ones (Table 21). On one hand, the cobalt-catalyzed oxidation of β-pinene **12** and 3-carene **3** mainly afforded the allylic mono-oxygenated products. At 37% conversion, β-pinene **12** was equally transformed with a high global selectivity of 95% into *trans*-pinocarveol **13**, pinocarvone **14**, myrtenal **15**, and myrtenol **16**, while 3-carene **3** gave several allylic ketones, such as 3-carene-5-one (46%), 2-carene-4-one (14%) and 3-carene-2-one (11%). On the other hand, limonene **2** and α-pinene **1** gave allylic oxidation products and epoxides, with a molar ratio of allylic products vs. epoxides of 1.4 and 2–2.5, respectively.

In 2007, Kholdeeva immobilized on hydrothermally stable silicates, such as mesoporous cellular foams (MCFs) or mesostructured materials (SBA-15), a cobalt-substituted polyoxometalate ($[Bu_4N]_4H[PW_{11}Co(H_2O)O_{39}]$) via an electrostatic binding between the CoPOM and the amino-modified support [75]. FTIR and DRS-UV-vis (Diffuse reflectance spectroscopy) analyses prove the retention of the CoPOM on the support. In aerobic conditions, the oxidation of α-pinene **1** could be oriented toward the formation of allylic oxidation products, such as verbenone **8** and verbenol **32** with selectivities up to 70% (at 20% conversion) or to epoxide as major product, using 2-methylpropanal as co-oxidant (Table 22).

Table 21. Aerobic oxidation of terpenic olefins with Co- and Mn-substituted ferrites [a] (adapted from reference [74]).

Entry	Substrate	Catalyst	Conversion [b] (%)	S_{allyl} [b] (%)	S_{Epox} [b] (%)	TON [c]
1a		$Co-Fe_3O_4$	40	64	26	100
1b	**1**	$Mn-Fe_3O_4$	32	60	28	83
2a		$Co-Fe_3O_4$	37	95	-	103
2b	**12**	$Mn-Fe_3O_4$	30	94	-	78
3a		$Co-Fe_3O_4$	40	71	4	111
3b	**3**	$Mn-Fe_3O_4$	30	67	5	78
4a		$Co-Fe_3O_4$	40	47	34	111
4b	**2**	$Mn-Fe_3O_4$	38	48	33	98

[a] Conditions: Catalyst (1.2 wt%), 18 mmol substrate, 60 °C, 1 bar O_2, 7 h. [b] Determined by GC. [c] TON defined as moles of the substrate converted/moles of metal (Co or Mn).

Table 22. Effect of 2-methylpropanal on the aerobic oxidation of α-pinene **1** with cobalt-substituted polyoxometalate on amino-modified supports [a] (adapted from reference [75]).

| Entry	Catalyst	With 2-Methylpropanal at 25 °C [b]			Without 2-Methylpropanal at 50 °C		
		Conv. (%)	Yield [c] (%)		Conv. (%)	Yield [c] (%)	
			Campholenic Aldehyde	α-Pinene Epoxide		Verbenone	Verbenol
1	Co-POM	77	8 (10)	67 (87)	45	16 (36)	11 (24)
2	Co-POM/NH_2-SBA-15	95	15 (16)	72 (76)	46	12 (26)	6 (13)
3	Co-POM/NH_2-MCF	96 [d]	8 (8)	90 (94)	43	10 (23)	6 (14)

[a] Conditions: Catalyst (6×10^{-4} mmol), α-pinene (0.1 mmol), 1 bar O_2, CH_3CN, 1 h. [b] 2-methylpropanal (0.4 mmol). [c] GC yield based on initial α-pinene (inside parentheses, CG yield based on α-pinene consumed). [d] After 2 h.

Similarly, cobalt-containing MCM-41 catalysts were prepared by direct incorporation of cobalt species into the support by a hydrothermal treatment [76]. Characterization showed that the metal was mainly introduced on the surface as isolated Co^{2+} species. This catalyst was efficient for the mild and solventless aerobic oxidation of isolongifolene **50** into the corresponding ketone **51** with selectivity up to 90% (Scheme 13).
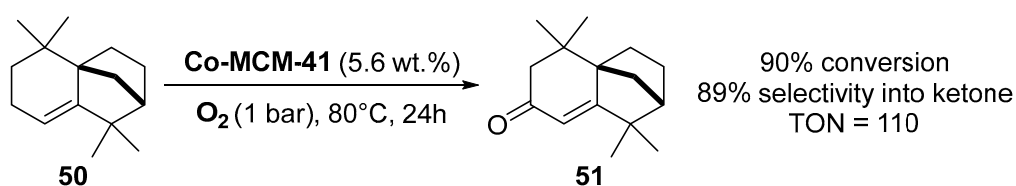
Scheme 13. Aerobic allylic oxidation of isolongifolene in the presence of Co-MCM41.
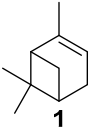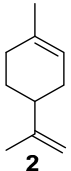
Originally, reeds (*Phragmites communis*) leaves were used as an eco-respectful template to synthesize cobalt-doped mesoporous silica (Co/SiO$_2$/PC) [77]. This catalyst is efficient for the mild aerobic oxidation of limonene **2**, with a complete conversion in 18 h and a 40% selectivity in carvone **9** in acetic anhydride (Figure 14). Hot catalyst filtration experiments proved the heterogeneous nature of the material Co/SiO$_2$/PC, which can be reusable over three runs.
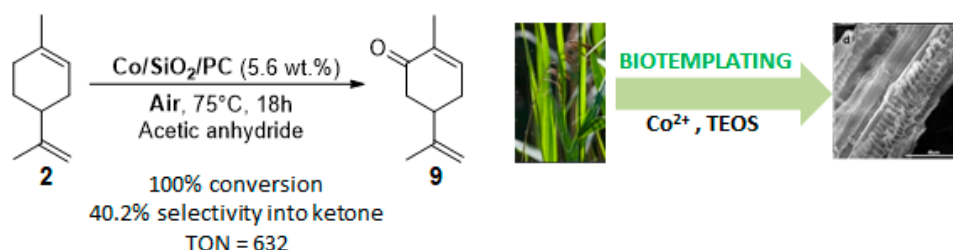
Figure 14. Co/SiO$_2$/PC-catalyzed allylic oxidation of limonene **2** (adapted from reference [77]).

Nickel catalyst. Chloromethylated polystyrene-crosslinked with 2-aminopyridine was used as a macromolecular support for anchoring nickel(II) complex [78]. The obtained catalyst proved to be efficient and reusable for the oxidation of two terpenic olefins (α-pinene **1** and limonene **2**) in the presence of *t*-BHP in aqueous solution with high TurnOver Frequencies (Table 23).

**Table 23.** Polymer-anchored nickel(II) complex in allylic oxidation of model terpenes [a] (adapted from reference [78]).

Entry	Substrate	Conversion [b] (%)	Product (Selectivity %) [b]	TOF (h^{-1})
1	**1**	69	Verbenone (76) Verbenol (24)	205.4
2	**2**	58	Carvone (87) Carveol (12)	172.6

[a] Reaction conditions: Catalyst (0.05 g), substrate (5 mmol), t-BHP (10 mmol), H$_2$O (10 mL), 60 °C, 12 h. [b] Determined by GC and GC-MS.

Copper catalysts. Copper catalysts are also relevant for the allylic oxidation of terpenic olefins. For instance, activated carbon-supported CuCl$_2$ (CuCl$_2$/AC) was used in the liquid phase oxidation of (+)-3-carene **3** with *tert*-butylhydroperoxide and dioxygen [79]. After optimization of the reaction conditions (45 °C, 3 eq. *t*-BHP), the substrate was completely converted into (−)-3-carene-2,5-dione **10** with a 78% selectivity in 12 h (Scheme 14). The optimized conditions were extended to α-pinene **1**, leading to the formation of verbenone **8** with a 28% yield at 40 °C and up to 77% at 70 °C.
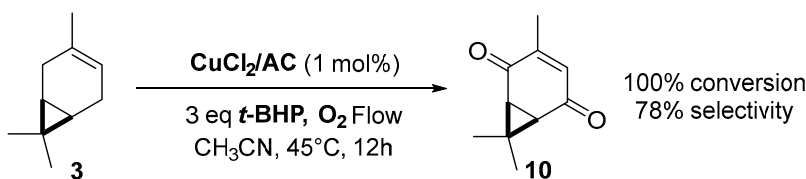
Scheme 14. Synthesis of (−)-3-carene-2,5-dione via a Cu-catalyzed-oxidation process (adapted from reference [79]).

In 2014, the team of Guerra developed a novel process for the allylic oxidation of alkenes, catalyzed by a copper-aluminum mixed oxide (Cu-Al Ox), with *tert*-butylhydroperoxide and a carboxylic acid [80]. In this study, the monoterpenic β-pinene **12** and the sesquiterpenic valencene **45** were investigated. In the presence of alkylated or aromatic carboxylic acids, the reaction yielded the corresponding allylic esters, while allylic alcohol or ketone were obtained with *L*-Proline. An overview of the results is detailed in Scheme 15. Interestingly, the authors developed experimental (DoE) statistical methodology to optimize the oxidation of valencene **45**.
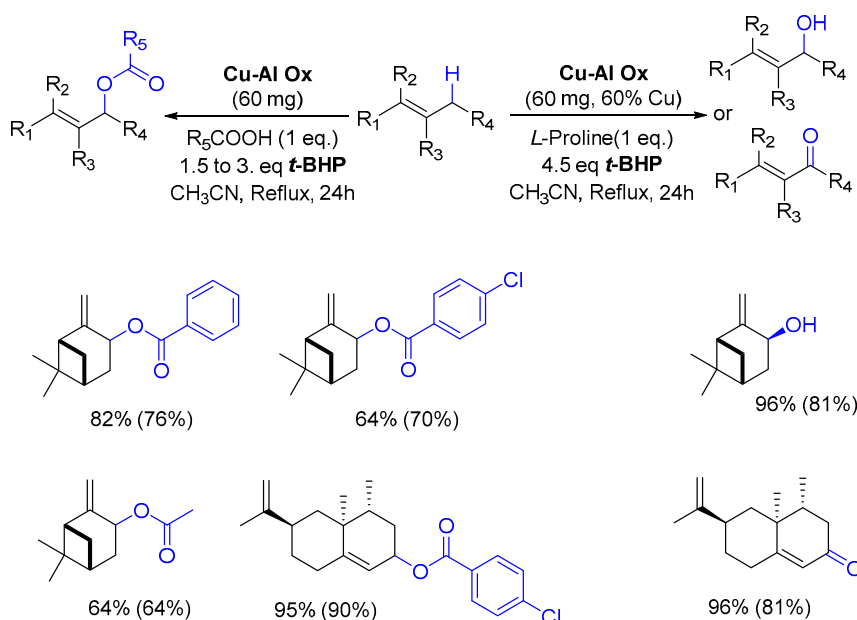
Scheme 15. Cu-Al Ox-catalyzed oxidation of terpenes with carboxylic acid or *L*-proline. (adapted from reference [80]). GC yields (isolated yield) are given.

Vanadium catalysts. Supported vanadium catalysts are also pertinent candidates for the upgrading of terpenic olefins into oxyfunctionalized compounds. First, nickel phosphate molecular sieves (VSB-5), whose structural properties can be easily tunable by isomorphous substitution of transition metal ions in the VSB-5 framework, proved to be relevant supports [81]. Thus, Timofeeva et al. studied the insertion of vanadium ions, which could increase the surface acidity [82]. The vanadium-containing nickel phosphate molecular sieves (V-VSB-5) were hydrothermally prepared with microwave irradiation using $NiCl_2·6H_2O$, $VOSO_4·xH_2O$ and *ortho*-phosphoric acid (H_3PO_4, 85%) as nickel, vanadium, and phosphorus sources. From XPS and DR-UV-Vis spectroscopy, the presence of both V^{4+} and V^{5+} species were proved. Moreover, the effect of vanadium content on surface acidity was studied through adsorption of pyridine and phenolic red. An increase in the strength of Brönsted acid sites was observed at higher vanadium content. The catalysts with various metal contents were tested in the oxidation of α-pinene **1** with molecular oxygen (1 bar) in acetonitrile (Table 24). The allylic oxidation of α-pinene **1** over V-VSB-5 catalysts leads to the major formation of allylic products (verbenone **8** and verbenol **32**), combined with epoxidation ones (α-pinene epoxide **5**, α-campholene aldehyde **26** and

trans-carveol **17**). Moreover, the vanadium content in the material influenced the conversion, as well as the distribution of products. Higher amounts of vanadium enhanced the catalytic activity, up to 18% conversion with 1.7% vanadium content, and the campholenic aldehyde/*trans*-carveol ratio. As already reported in the literature, the isomerization of α-pinene oxide **5** leading to campholenic acid is favored on Lewis acid sites, while *trans*-carveol formed over Brönsted sites.

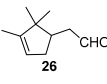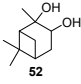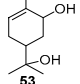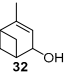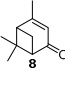**Table 24.** Oxidation of α-pinene over V-VSB-5 catalysts. Influence of the Brönsted and Lewis sites [a] (adapted from reference [82]).

Entry	Catalyst	N_{LAS}/N_{BAS} (mol·mol^{-1}) [b]	Conv. [c] (%)	Selectivity [c] (mol %)	
				Epoxidation	Allylic Oxidation
1	VSB-5	1.8	3	38	48
2	1.1% V-VSB-5	1.3	12	38	45
3	1.7% V-VSB-5	0.9	18	35	48

[a] Reaction conditions: Catalyst (20 mg), α-pinene (0.1 mmol), 1 bar O_2, CH_3CN, 60 °C, 5 h. [b] Brönsted and Lewis acidity were determined by FTIR spectroscopy using pyridine as probe molecules. [c] Determined by GC analyses.

Molecular sieves based on a MCM-41 structure were also used to support vanadium species, using $VO(SO_4) \cdot H_2O$ as metal precursor, cetyltrimethylammonium bromide salt as template and tetraethoxysilane as silica source [83]. UV-Vis-DR and FT-IR Raman studies proved the presence of two types of $V^{\delta+}$ species, as well as oligonuclear nanoclusters ($V^{\delta+} \cdots O^{\delta-} \cdots V^{\delta+}$), which could be found either inside or also on the wall of the support. The various V-M(x) catalysts, with x being the Si/V molar ratio, were tested in the oxidation of α-pinene **1** with hydrogen peroxide (Table 25). Vanadium ions proved to be the active species since no reaction occurred in their absence. A high selectivity in ketone **8** up to 46% was observed with V-M(240) catalyst (Entry 3). Interestingly, although an increased H_2O_2 conversion is observed at high metal content (Entry 1), a higher efficiency is obtained with V-M(240), probably due to the formation of extra-framework nanoclusters and vanadium oligomers, which are responsible for H_2O_2 decomposition into water. Finally, the catalyst was easily recycled over four runs with good catalytic performances.

Table 25. Oxidation of α-pinene **1** over V-M(x) catalysts. Influence of the metal content [a] (adapted from reference [83]).

Entry	Catalyst	Conv. [b] (%)	H_2O_2 Conv. [c] (mol %)	H_2O_2 Efficiency [d] (mol %)	Selectivity [e] (%)				
					26	52	53	32	8
1	V-M(20)	10	91.3	38.3	33.7	12.2	21.8	4.1	9.1
2	V-M(60)	12.8	84.5	53.2	13.4	15.9	36.3	11.4	7.8
3	V-M(240)	11.4	79.7	57.2	24.1	3.7	5.3	14.1	46.0

[a] Reaction conditions: Catalyst (9 g·L^{-1}), α-pinene (0.17 mmol), H_2O_2 (1.79 mmol), CH_3CN, 70 °C, 7 h. [b] Ratio of converted species to initial concentration. [c] Measured by iodometric titration. [d] Moles of products formed/moles of H_2O_2 converted. [e] Defined as moles product/moles total products (mol product/ mol total products) × 100.

Recently, several oxidized metal complexes (VO^{IV}, Mn^{II}, Fe^{II}, Co^{II}, Ni^{II} and Cu^{II}), modified by a Schiff base ligand, namely HMIMMPP for 4-(((2-hydroxy-5-methylphenyl)imino)methyl)-3-methyl-1-phenyl-1H-pyrazol-5-ol, were entangled in the zeolite Y matrix through a two-step process (Figure 15a) and compared in the oxidation of α-pinene **1** with *tert*-butylhydroperoxide in acetonitrile (Figure 15b) [84]. The reaction gave verbenol **32** and verbenone **8** as major products, with small amounts of myrtenol (6–7%), campholene aldehyde (3–4%) and epoxide (2–4%) as co-products. The conversion is influenced by the metal, increasing in the following order: Mn < Fe < Ni < Cu < Co < VO.

The [VO(HMIMMPP)(H₂O)]-Y catalyst showed the highest conversion (45.3%) with a 40.7% selectivity in ketone. This process could also be considered as eco-responsible with a good catalyst's recycling.
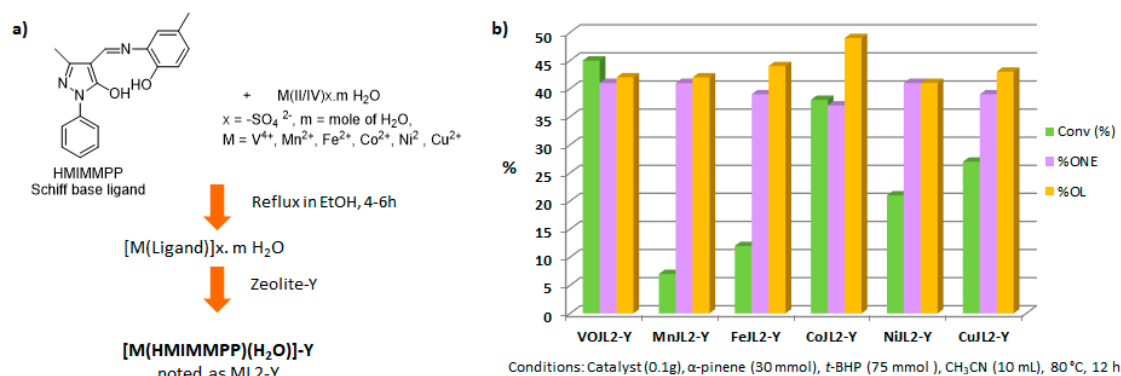
Figure 15. (**a**) Synthesis of zeolite-Y entagled M(II/IV) complexes. (**b**) Comparison of their catalytic activities in oxidation of α-pinene **1** (adapted from reference [85]).

**Titania catalyst.** In 2008, Casuscelli reported Ti-MCM-41, prepared by hydrothermal synthesis, as catalyst for the α-pinene oxidation using hydrogen peroxide [85]. From UV-vis analyses, the active species are present in tetrahedrally coordinated Ti⁴⁺ ions. An increase in the titania content did not improve the conversion, due to a rapid consumption of the oxidant at the early stage of the reaction. The yield of oxidation products, mainly verbenone **8**, verbenol **32** and campholenic aldehyde **26**, was increased with an extra dose of oxidant after 1 h of reaction (Scheme 16). As previously reported, the selectivity with Ti-MCM-41 catalyst, prepared by hydrothermal synthesis, differs from those prepared by a post-synthetic approach, which are in favor of epoxides [42].
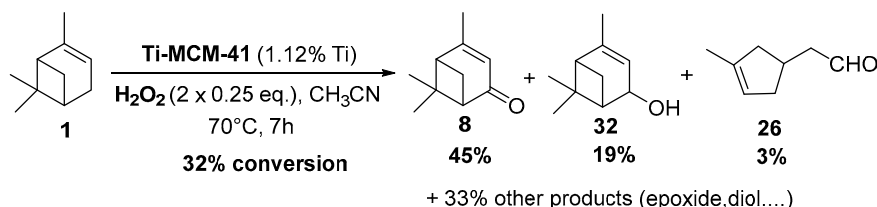
Scheme 16. Ti-MCM41-catalyzed allylic oxidation of α-pinene (adapted from reference [85]).

3.3. Aqueous Suspensions of Ruthenium Nanoparticles

Nanometer-sized metal particles with a behavior located at the interface between molecular complexes and heterogeneous catalysts, are considered as relevant catalysts owing to their novel surface reactivities and thus original activities and/or selectivities for many reactions [86]. Although Co₃O₄ nanoparticles in organic media (DMF) were reported for the epoxidation of α-pinene **1** [87], the use of metallic nanoparticles finely dispersed in water, as a cheap, available and benign solvent [88,89], has not been described yet. In that context, our team have very recently developed aqueous suspensions of ruthenium (0) nanoparticles, stabilized with a hydroxyethylammonium salt (HEA16Cl) and possessing sizes around 2.0 nm, for the mild allylic oxidation of α-pinene, with *tert*-butylhydroperoxide in neat water (Figure 16) [90]. After optimization of the reaction conditions, verbenone **8** was obtained as major product with a yield up to 41%, alongside 2-hydroxy-3-pinanone **54** (<7%) as co-product. The sequential addition of the oxidant (2 × 1.5 equiv.) enables to increase the ketone yield.
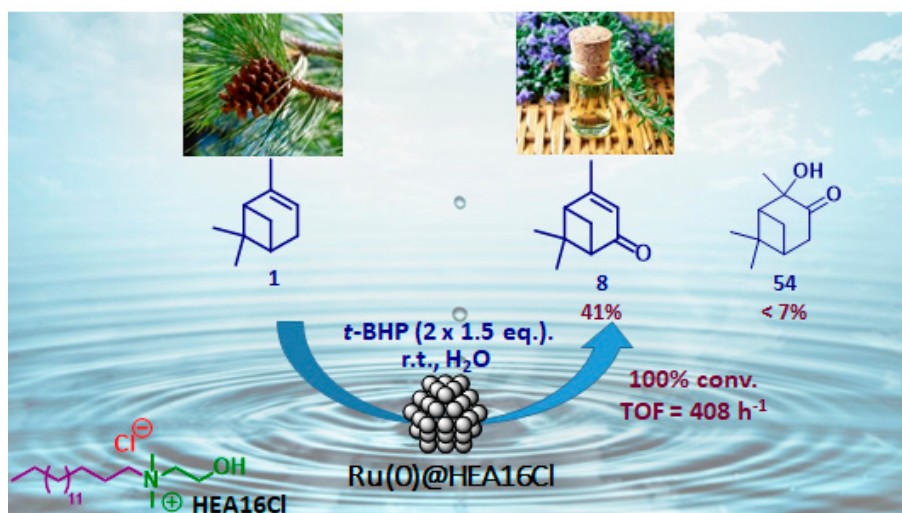
Figure 16. Ammonium surfactant-stabilized ruthenium nanoparticles for oxidation of α-pinene **1** in neat water (adapted from reference [90]).

This catalytic system was extended to valencene **45**, leading to the formation of the corresponding nootkatone **46** with a 60% isolated yield in water, at room temperature (Scheme 17). This result is quite similar to the one obtained with a Cu-Al-Ox catalyst used in acetonitrile at 80 °C [78]. This oxyfunctionalized molecule constitutes an important flavoring constituent due its citrusy, woody, peely, and grapefruitlike aroma profile [91] and is also a natural insect repellent [92].
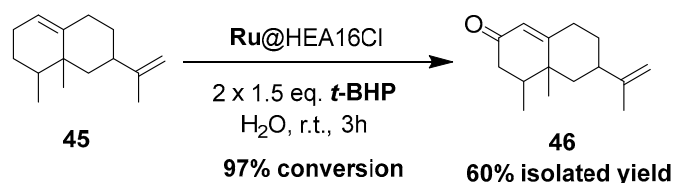
Scheme 17. Production of nootkatone, catalyzed by ammonium-protected ruthenium nanoparticles.

3.4. Conclusions

Allylic oxidations, which enable the transformation of olefin compounds into allyl alcohols or α,β-unsaturated ketones, constitute a relevant Csp^3-H functionalization, afforded synthetic and value-added target molecules for flavoring and pharmaceutical industries. Terpenes, available from renewable sources, are relevant starting materials for these reactions. The bibliographic study, detailed in this part, showed that various catalysts, either molecular complexes or heterogeneous catalysts, can be used for the allylic oxidations of various terpenic olefins. The Figure 17 gives a comparison of different catalysts used for the allylic oxidation of α-pinene **1**, one of the most studied terpenic olefin. The reaction is usually carried out in organic solvents (dichloromethane, acetone, acetonitrile), in the presence of various oxidants such as *tert*-butylhydroperoxide (*t*-BHP), hydrogen peroxide (H_2O_2), as well as dioxygen. In many cases, the allylic product, verbenone **8**, was obtained with low to medium yields, from 10 to 55%. However, two heterogeneous catalysts lead to yields up to 80% in **8**. First, a mechanochemically activated iron-pillared montmorillonite material allowed a complete conversion of the substrate with an 84% isolated yield in verbenone **8**. Nevertheless, this reaction proceeded with large amounts of oxidant (10 eq.) and in 50 h, that is to say more than two days [68]. In 2013, a hierarchically ordered porous lotus-shaped nanostructured MnO_2 catalyst was found pertinent for this transformation, with an 82% yield in verbenone **8** [70]. However, the reproducible synthesis of this catalyst remains complex.
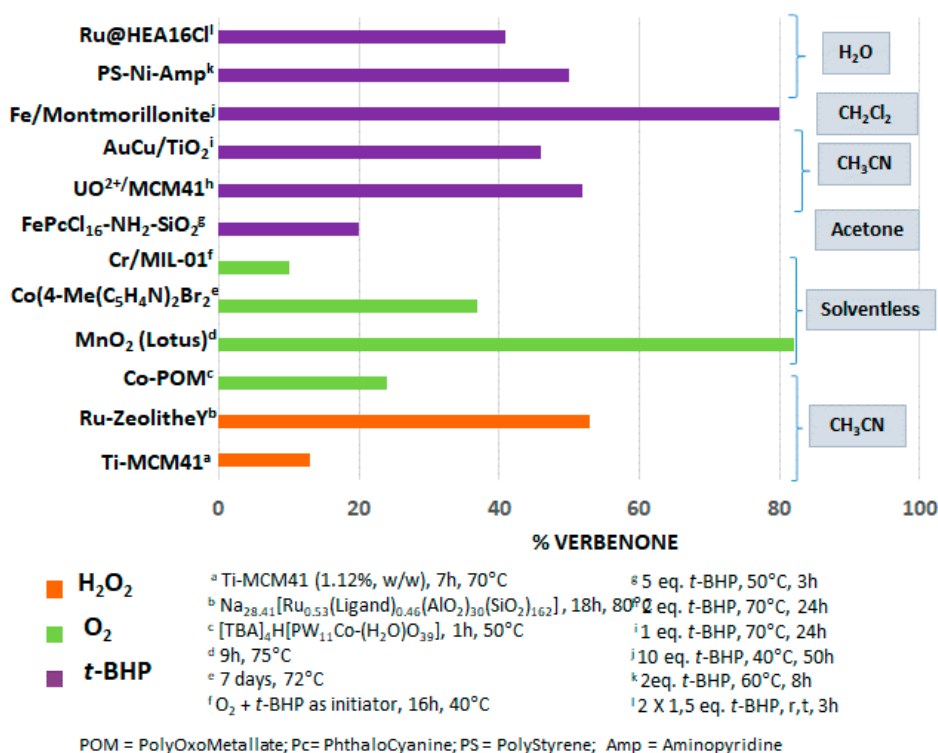
Figure 17. Comparison of various catalysts for the allylic oxidation of α-pinene **1**.

Although many works have been carried out for the allylic oxidation of olefinic terpenes, most processes still suffer from some drawbacks such as moderate conversions and/or selectivities, sophisticated catalytic systems, toxic organic solvent as well as huge amounts of oxidant, long reaction times and difficult catalyst's recycling. It is noteworthy to underline that two examples for the allylic oxidation of α-pinene **1** were carried out in water as a green reaction media, with polymer-supported nickel catalyst [41] or with aqueous suspensions of ruthenium nanoparticles [90].

4. Conclusions and Perspectives

Olefinic terpenes constitute a promising source of abundant and cheap biorenewables, whose upgrading could afford huge economic benefits, with wide applications in many chemical industries. The most representative and viable sources of terpenes are the turpentine resins extracted from coniferous trees [93] and the essential oils from citrics [94]. Among the various catalytic chemical processes for the valorization of these agro-resources [95], oxidation reactions represent a relevant methodology for the upgrading of some usual terpenes into value-added oxyfunctionalized chemicals for the pharmaceutical, perfumery, and flavoring industries. According to the nature of the catalysts and/or the reaction conditions, the oxidation reaction could lead to the formation of either epoxide via the epoxidation of the double bond or allylic oxidation products via the functionalization of the Csp^3-H bond.

In the literature, many catalysts, either molecular complexes or heterogeneous materials, based on noble metals (for instance ruthenium, gold, palladium species) but also on first row transition metals (such as cobalt, vanadium, manganese, nickel, etc.), were used for the oxidation of model terpenes. Classically, various oxidants such as organic ones (*t*-BHP or peracetic acid) or greener ones—for instance hydrogen peroxide (H_2O_2) or molecular dioxygen (O_2)—were used. Heterogeneous catalytic approaches are generally industrially preferred, compared to homogeneous ones, with regard to the associated benefits, such as easy separation of the reaction products and good durability and recyclability of the catalysts. Nevertheless, in most cases, low to medium yields were obtained, and high levels of selectivity remain difficult to reach with complex reaction mixtures due to the sensitivity

of the products. Moreover, most of the oxidation processes still suffer from various drawbacks, such as the use of too sophisticated catalysts, toxic organic solvents, and high amounts of oxidants, alongside long reaction times and difficult catalyst recovery. Consequently, the development of new processes for industrial plants still constitutes a target in this field.

Although great achievements have been accomplished on the upgrading of terpenic olefins through oxidation processes, further improvements with new catalytic methodologies are still required for industrially large-scaled and economical production of the value-added oxyfunctionalized terpenic olefins such as epoxides or α,β-unsaturated ketones. Thus, we can highlight some strategic points, such as (1) the design of cost-effective catalysts, which could be efficient for a large variety of terpenes with very high level of selectivity; (2) a better understanding of the mechanism insights and structure-activity relationships to favor the reaction selectivity; (3) control of the catalyst's acidity or basicity to avoid the formation of co-products; (4) the design of a easy and low-cost approach for the large-scale production of oxyfunctionalized products with a reduced environmental footprint; and finally (5) besides noble metals, a preference for the use of cheap and abundant first-row transition metals. Continuous investigations of more efficient and suitable nanoparticle-based catalysts are still highly demanded, with regard to their new surface reactivities and their potential recyclabilities under adapted conditions, and the could also be of great value for industrial applications. This research field on nanoparticles seems to be under-exploited, and few pertinent results were described in the literature review. New developments of nanocatalysts in terms of shape, structure, and morphologies providing new surface reactivities could be suitable and benefit for relevant selectivities.

This critical mini-review provides a large variety of studies for the catalytic oxidative upgrading of renewable terpenic olefins and should be helpful to develop more efficient methodologies for these relevant transformations.

Conflicts of Interest: The authors declare no conflict of interest.

References and Note

1.　Berger, R.G. *Flavours and Flagrances—Chemistry, Bioprocessing and Sustainability*; Springer: Berlin/Heidelberg, Germany, 2007.

2.　Ciriminna, R.; Lomeli-Rodriguez, M.; Demma Cara, P.; Lopez-Sanchez, J.A.; Pagliaro, M. Limonene: A versatile chemical of the bioeconomy. *Chem. Commun.* **2014**, *50*, 15288–15296. [CrossRef]

3.　Surburg, H.; Panten, J. *Common Fragrance and Flavor Materials: Preparation, Properties and Uses*, 5th ed.; Wiley-VCH: Weinheim, Germany, 2006.

4.　Schwab, W.; Fuchs, C.; Huang, F.-C. Transformation of terpenes into fine chemicals. *Eur. J. Lipid Sci. Technol.* **2013**, *115*, 3–8. [CrossRef]

5.　Swift, K.A.D. Catalytic Transformations of the Major Terpene Feedstocks. *Top. Catal.* **2004**, *27*, 143–155. [CrossRef]

6.　Ravasio, N.; Zaccheria, F.; Guidotti, M.; Psaro, R. Mono- and Bifunctional Heterogeneous Catalytic Transformation of Terpenes and Terpenoids. *Top. Catal.* **2004**, *27*, 157–168. [CrossRef]

7.　Golets, M.; Ajaikumar, S.; Mikkola, J.-P. Catalytic Upgrading of Extractives to Chemicals: Monoterpenes to "EXICALS". *Chem. Rev.* **2015**, *115*, 3141–3169. [CrossRef] [PubMed]

8.　Anastas, P.T.; Crabtree, R.H. *Green Chemistry*; Wiley-VCH: Weinheim, Germany, 2009.

9.　Busacca, C.A.; Fandrick, D.R.; Song, J.J.; Senanayake, C.H. The Growing Impact of Catalysis in the Pharmaceutical Industry. *Adv. Synth. Catal.* **2011**, *353*, 1825–1864. [CrossRef]

10.　Bicas, J.L.; Dionísio, A.P.; Pastore, G.M. Bio-oxidation of Terpenes: An Approach for the Flavor Industry. *Chem. Rev.* **2009**, *109*, 4518–4531. [CrossRef] [PubMed]

11. Caovilla, M.; Caovilla, A.; Pergher, S.B.C.; Esmelindro, M.C.; Fernandes, C.; Dariva, C.; Bernardo-Gusmão, K.; Oestreicher, E.G.; Antunes, O.A.C. Catalytic oxidation of limonene, α-pinene and β-pinene by the complex [FeIII(BPMP)Cl(μ-O)FeIIICl₃] biomimetic to MMO enzyme. *Catal. Today* **2008**, *133*, 695–698. [CrossRef]

12. Robles-Dutenhefner, P.A.; Brandão, B.B.N.S.; De Sousa, L.F.; Gusevskaya, E.V. Solvent-free chromium catalyzed aerobic oxidation of biomass-based alkenes as a route to valuable fragrance compounds. *Appl. Catal. A* **2011**, *399*, 172–178. [CrossRef]

13. Adolfsson, H. Transition metal-catalyzed epoxidation of alkenes. In *Modern Oxidation Methods*, 2nd ed.; Baeckvall, J.-E., Ed.; Wiley-VCH Verlag GmbH & Co. KGaA: Weinheim, Germany, 2010; pp. 37–84.

14. Yudin, A.K. *Aziridines and Epoxides in Organic Synthesis*; Wiley-VCH Verlag GmbH & Co. KGaA: Weinheim, Germany, 2006.

15. Gusevskaya, E.; Robles-Dutenhefner, P.A.; Ferreira, V.C.M.S. Palladium-catalyzed oxidation of bicyclic monoterpenes by hydrogen peroxide. *Appl. Catal. A* **1998**, *174*, 177–186. [CrossRef]

16. De Oliveira, A.A.; Da Silva, M.L.; Da Silva, M.J. Palladium-Catalysed Oxidation of Bicycle Monoterpenes by Hydrogen Peroxide in Acetonitrile Solutions: A Metal Reoxidant-Free and Environmentally Benign Oxidative Process. *Catal. Lett.* **2009**, *130*, 424–431. [CrossRef]

17. Yamazaki, S. An effective procedure for the synthesis of acid-sensitive epoxides: Use of 1-methylimidazole as the additive on methyltrioxorhenium-catalyzed epoxidation of alkenes with hydrogen peroxide. *Org. Biomol. Chem.* **2010**, *8*, 2377–2385. [CrossRef] [PubMed]

18. Yamazaki, S. An efficient organic solvent-free methyltrioxorhenium-catalyzed epoxidation of alkenes with hydrogen peroxide. *Tetrahedron* **2008**, *64*, 9253–9257. [CrossRef]

19. Egorova, K.S.; Ananikov, V.P. Toxicity of Metal Compounds: Knowledge and Myths. *Organometallics* **2017**, *36*, 4071–4090. [CrossRef]

20. Manganese price in 2018 was 2.06 \$/kg.

21. Enghag, P. *Encyclopedia of the Elements*; Wiley-VCH Verlag GmbH & Co. KGaA: Weinheim, Germany, 2004.

22. Cubillos, J.; Vásquez, S.; Montes de Correa, C. Salen manganese(III) complexes as catalysts for R-(+)-limonene oxidation. *Appl. Catal. A* **2010**, *373*, 57–65. [CrossRef]

23. Dong, J.J.; Saisaha, P.; Meinds, T.G.; Alsters, P.L.; Ijpeij, E.G.; Van Summeren, R.P.; Mao, B.; Fañanás-Mastral, M.; De Boer, J.W.; Hage, R. Oxidation of Alkenes with H_2O_2 by an in-Situ Prepared Mn(II)/Pyridine-2-carboxylic Acid Catalyst and the Role of Ketones in Activating H_2O_2. *ACS Catal.* **2012**, *2*, 1087–1096. [CrossRef]

24. Mandelli, D.; Kozlov, Y.N.; Da Silva, C.A.R.; Carvalho, W.A.; Pescarmona, P.P.; Cella, D.D.A.; De Paiva, P.T.; Shul'pin, G.B. Oxidation of olefins with H_2O_2 catalyzed by gallium(III) nitrate and aluminum(III) nitrate in solution. *J. Mol. Catal. A* **2016**, *422*, 216–220. [CrossRef]

25. Novikov, A.S.; Kuznetsov, M.L.; Pombeiro, A.J.L.; Bokach, N.A.; Shul'pin, G.B. Generation of HO• Radical from Hydrogen Peroxide Catalyzed by Aqua Complexes of the Group III Metals $[M(H_2O)n]^{3+}$ (M = Ga, In, Sc, Y, or La): A Theoretical Study. *ACS Catal.* **2013**, *3*, 1195–1208. [CrossRef]

26. Kon, Y.; Ono, Y.; Matsumoto, T.; Sato, K. An Effective Catalytic Epoxidation of Terpenes with Hydrogen Peroxide under Organic Solvent-Free Conditions. *Synlett* **2009**, *2009*, 1095–1098. [CrossRef]

27. Clerici, M.G.; Kholdeeva, O.A. *Liquid Phase Oxidation via Heterogeneous Catalysis: Organic Synthesis and Industrial Applications*; Wiley: Hoboken, NJ, USA, 2013.

28. Bonon, A.J.; Kozlov, Y.N.; Bahú, J.O.; Filho, R.M.; Mandelli, D.; Shul'pin, G.B. Limonene epoxidation with H_2O_2 promoted by Al_2O_3: Kinetic study, experimental design. *J. Catal.* **2014**, *319*, 71–86. [CrossRef]

29. Cao, Y.; Li, Y.; Yu, H.; Peng, F.; Wang, H. Aerobic oxidation of -pinene catalyzed by carbon nanotubes. *Catal. Sci. Technol.* **2015**, *5*, 3935–3944. [CrossRef]

30. Yu, N.; Ding, Y.; Lo, A.-Y.; Huang, S.-J.; Wu, P.-H.; Liu, C.; Yin, D.; Fu, Z.; Yin, D.; Hung, C.-T. Gold nanoparticles supported on periodic mesoporous organosilicas for epoxidation of olefins: Effects of pore architecture and surface modification method of the supports. *Microporous Mesoporous Mater.* **2011**, *143*, 426–434. [CrossRef]

31. Betz, D.; Boland, W.; Hudson, A.; Jimenez-Aleman, G.H.; Kuhn, F.E. *The Handbook of Reagents for Organic Synthesis: Catalytic Oxidation Reagents*; Fuchs, P.L., Ed.; John Wiley & Sons Ltd.: Chichester, UK, 2013; Volumes 396–407.

32. Zhou, M.-D.; Jain, K.R.; Günyar, A.; Baxter, P.N.W.; Herdtweck, E.; Kühn, F.E. Bidentate Lewis Base Adducts of Methyltrioxidorhenium(VII): Ligand Influence on Catalytic Performance and Stability. *Eur. J. Inorg. Chem.* **2009**, *2009*, 2907–2914. [CrossRef]

33. Saladino, R.; Andreoni, A.; Neri, V.; Crestini, C. A novel and efficient catalytic epoxidation of olefins and monoterpenes with microencapsulated Lewis base adducts of methyltrioxorhenium. *Tetrahedron* **2005**, *61*, 1069–1075. [CrossRef]

34. Abu-Dief, A.M.; Mohamed, I.M.A. A review on versatile applications of transition metal complexes incorporating Schiff bases. *Beni-Suef Univ. J. Basic Appl. Sci.* **2015**, *4*, 119–133. [CrossRef]

35. Canali, L.C.; Sherrington, D. Utilisation of homogeneous and supported chiral metal(salen) complexes in asymmetric catalysis. *Chem. Soc. Rev.* **1999**, *28*, 85–93. [CrossRef]

36. Saikia, L.; Srinivas, D.; Ratnasamy, P. Comparative catalytic activity of Mn(Salen) complexes grafted on SBA-15 functionalized with amine, thiol and sulfonic acid groups for selective aerial oxidation of limonene. *Microporous Mesoporous Mater.* **2007**, *104*, 225–235. [CrossRef]

37. Oliveira, P.; Machado, A.; Ramos, A.M.; Fonseca, I.; Fernandes, F.M.B.; Rego, A.M.B.D.; Vital, J. MCM-41 anchored manganese salen complexes as catalysts for limonene oxidation. *Microporous Mesoporous Mater.* **2009**, *120*, 432–440. [CrossRef]

38. Qi, Y.; Luan, Y.; Yu, J.; Peng, X.; Wang, G. Nanoscaled Copper Metal–Organic Framework (MOF) Based on Carboxylate Ligands as an Efficient Heterogeneous Catalyst for Aerobic Epoxidation of Olefins and Oxidation of Benzylic and Allylic Alcohols. *Chem. Eur. J.* **2015**, *21*, 1589–1597. [CrossRef]

39. Lajunen, M.K. Co(II) catalysed oxidation of α-pinene by molecular oxygen: Part III. *J. Mol. Catal. A* **2001**, *169*, 33–40. [CrossRef]

40. Patil, M.V.; Yadav, M.K.; Jasra, R.V. Catalytic epoxidation of α-pinene with molecular oxygen using cobalt (II)-exchanged zeolite Y-based heterogeneous catalysts. *J. Mol. Catal. A* **2007**, *277*, 72–80. [CrossRef]

41. Islam, S.M.; Ghosh, K.; Molla, R.A.; Roy, A.S.; Salam, N.; Iqubal, M.A. Synthesis of a reusable polymer anchored cobalt(II) complex for the aerobic oxidation of alkyl aromatics and unsaturated organic compounds. *J. Organomet. Chem.* **2014**, *774*, 61–69. [CrossRef]

42. Marino, D.; Gallegos, N.G.; Bengoa, J.F.; Alvarez, A.M.; Cagnoli, M.V.; Casuscelli, S.G.; Herrero, E.R.; Marchetti, S.G. Ti-MCM-41 catalysts prepared by post-synthesis methods: Limonene epoxidation with H_2O_2. *Catal. Today* **2008**, *133*, 632–638. [CrossRef]

43. Rocha, G.M.S.R.O.; Domingues, R.M.A.; Simões, M.M.Q.; Silva, A.M.S. Catalytic activity of tetravalent metal phosphates and phosphonates on the oxidation of (+)-3-carene. *Appl. Catal. A* **2009**, *353*, 236–242. [CrossRef]

44. Selvaraj, M.; Kawi, S.; Park, D.W.; Ha, C.S. A Merit Synthesis of Well-Ordered Two-Dimensional Mesoporous Niobium Silicate Materials with Enhanced Hydrothermal Stability and Catalytic Activity. *J. Phys. Chem. C* **2009**, *113*, 7743–7749. [CrossRef]

45. Ivanchikova, I.D.; Maksimchuka, N.V.; Skobelev, I.Y.; Kaichev, V.V.; Kholdeeva, O.A. Mesoporous niobium-silicates prepared by evaporation-induced self-assembly as catalysts for selective oxidations with aqueous H_2O_2. *J. Catal.* **2015**, *332*, 138–148. [CrossRef]

46. Sundaravel, B.; Babu, C.M.; Vinodh, R.; SeogCha, W.; Jang, H.-T. Synthesis of campholenic aldehyde from α-pinene using bi-functional PrAlPO-5 molecular sieves. *J. Taiwan Instit. Chem. Eng.* **2016**, *63*, 157–165. [CrossRef]

47. Stekrova, M.; Kumar, N.; Mäki-Arvela, P.; Aho, A.; Linden, J.; Volcho, K.P.; Salakhutdinov, N.F.; Murzin, D.Y. Opening of monoterpene epoxide to a potent anti-Parkinson compound of para-menthane structure over heterogeneous catalysts. *React. Kinet. Mech. Catal.* **2013**, *110*, 449–458. [CrossRef]

48. Prat, D.; Hayler, J.; Wells, A. A survey of solvent selection guides. *Green Chem.* **2014**, *16*, 4546–4551. [CrossRef]

49. Mouret, A.; Leclercq, L.; Mühlbauer, A.; Nardello-Rataj, V. Eco-friendly solvents and amphiphilic catalytic polyoxometalate nanoparticles: A winning combination for olefin epoxidation. *Green Chem.* **2014**, *16*, 269–278. [CrossRef]

50. Da Silva, J.M.D.S.; Vinhado, F.S.; Mandelli, D.; Schuchardt, U.; Rinaldi, R. The chemical reactivity of some terpenes investigated by alumina catalyzed epoxidation with hydrogen peroxide and by DFT calculations. *J. Mol. Catal. A* **2006**, *252*, 186–193. [CrossRef]

51. Weidmann, V.; Maison, W. Allylic Oxidations of Olefins to Enones. *Synthesis* **2013**, *45*, 2201–2221.

52. Gonçalves, J.A.; Bueno, A.C.; Gusevskaya, E.V. Palladium-catalyzed oxidation of monoterpenes: Highly selective syntheses of allylic ethers from limonene. *J. Mol. Catal. A* **2006**, *252*, 5–11. [CrossRef]

53. Parreira, L.A.; Menini, L.; Gusevskaya, E.V. Palladium catalyzed oxidation of renewable terpenes with molecular oxygen: Oxidation of -bisabolol under chloride-free conditions. *Catal. Sci. Technol.* **2014**, *4*, 2016–2022. [CrossRef]

54. Catino, A.J.; Forslund, R.E.; Doyle, M.P. Dirhodium (II) Caprolactamate: An Exceptional Catalyst for Allylic Oxidation. *J. Am. Chem. Soc.* **2004**, *126*, 13622–13623. [CrossRef]

55. McLaughlin, E.C.; Choi, H.; Wang, K.; Chiou, G.; Doyle, M.P. Allylic Oxidations Catalyzed by Dirhodium Caprolactamate via Aqueous *tert*-Butyl Hydroperoxide: The Role of the *tert*-Butylperoxy Radical. *J. Org. Chem.* **2009**, *74*, 730–738. [CrossRef]

56. Zalatan, D.N.; Du Bois, J. Understanding the Differential Performance of Rh$_2$(esp)$_2$ as a Catalyst for C−H Amination. *J. Am. Chem. Soc.* **2009**, *131*, 7558–7559. [CrossRef]

57. Wang, Y.; Kuang, Y.; Wang, Y. Rh$_2$(esp)$_2$-catalyzed allylic and benzylic oxidations. *Chem. Commun.* **2015**, *51*, 5852–5855. [CrossRef]

58. Kholdeeva, O.A. Liquid-phase selective oxidation catalysis with metal-organic frameworks. *Catal. Today* **2016**, *278*, 22–29. [CrossRef]

59. Maksimchuk, N.V.; Kovalenko, K.A.; Fedin, V.P.; Kholdeeva, O.A. Heterogeneous Selective Oxidation of Alkenes to α,β- Unsaturated Ketones over Coordination Polymer MIL-101. *Adv. Synth. Catal.* **2010**, *352*, 2943–2948. [CrossRef]

60. Selvaraj, M.; Kandaswamy, M.; Park, D.W.; Ha, C.S. Highly efficient and clean synthesis of verbenone over well ordered two-dimensional mesoporous chromium silicate catalysts. *Catal. Today* **2010**, *158*, 286–295. [CrossRef]

61. Skobelev, I.Y.; Kovalenko, K.A.; Fedin, V.P.; Sorokin, A.B.; Kholdeeva, O.A. Allylic oxdation of alkenes with molecular oxygen catalyzed by porous coordination polymers Fe-MIL-101 and Cr-MIL-101. *Kinet. Catal.* **2013**, *54*, 607–614. [CrossRef]

62. Skobelev, I.Y.; Sorokin, A.B.; Kovalenko, K.A.; Fedin, V.P.; Kholdeeva, O.A. Solvent-free allylic oxidation of alkenes with O$_2$ mediated by Fe- and Cr-MIL-101. *J. Catal.* **2013**, *298*, 61–69. [CrossRef]

63. Kholdeeva, O.A.; Skobelev, I.Y.; Ivanchikova, I.D.; Kovalenko, K.A.; Fedin, V.P.; Sorokin, A.B. Hydrocarbon oxidation over Fe- and Cr-containing metal-organic frameworks MIL-100 and MIL-101–a comparative study. *Catal. Today* **2014**, *238*, 54–61. [CrossRef]

64. Godhani, D.R.; Nakum, H.D.; Parmar, D.K.; Mehta, J.P.; Desai, N.C. Zeolite Y encaged Ru(III) and Fe(III) complexes for oxidation of styrene, cyclohexene, limonene, and α-pinene: An eye-catching impact of H$_2$SO$_4$ on product selectivity. *J. Mol. Catal. A* **2017**, *426*, 223–237. [CrossRef]

65. Ajaikumar, S.; Ahlkvist, J.; Larsson, W.; Shchukarev, A.; Leino, A.R.; Kordas, K.; Mikkola, J.P. Oxidation of α-pinene over gold containing bimetallic nanoparticles supported on reducible TiO$_2$ by deposition-precipitation method. *Appl. Catal. A* **2011**, *392*, 11–18. [CrossRef]

66. Młodzik, J.; Wróblewska, A.; Makuch, E.; Wróbel, R.J.; Michalkiewicz, B. Fe/EuroPh catalysts for limonene oxidation to 1,2-epoxylimonene, its diol, carveol, carvone and perillyl alcohol. *Catal. Today* **2016**, *268*, 111–120. [CrossRef]

67. Becerra, J.-A.; González, L.-M.; Villa, A.-L. Kinetic study of α-pinene allylic oxidation over FePcCl16-NH$_2$-SiO$_2$ catalyst. *J. Mol. Catal. A* **2016**, *423*, 12–21. [CrossRef]

68. Romanenko, E.P.; Taraban, E.A.; Tkachev, A.V. Catalytic oxidation of α-pinene with *tert*-butyl hydroperoxide in the presence of Fe-pillared montmorillonite. *Russ. Chem. Bull.* **2006**, *55*, 993–998. [CrossRef]

69. Serra, S. MnO$_2$/TBHP: A Versatile and User-Friendly Combination of Reagents for the Oxidation of Allylic and Benzylic Methylene Functional Groups. *Eur. J. Org. Chem.* **2015**, *2015*, 6472–6478. [CrossRef]

70. Pal, P.; Pahari, S.K.; Giri, A.K.; Pal, S.; Bajaj, H.C.; Panda, A.B. Hierarchically order porous lotus shaped nano-structured MnO$_2$ through MnCO$_3$: Chelate mediated growth and shape dependent improved catalytic activity. *J. Mater. Chem. A* **2013**, *1*, 10251–10258. [CrossRef]

71. Lajunen, M.; Koskinen, A.M.P. Co(II)-catalysed allylic oxidation of α-pinene by molecular oxygen; synthesis of verbenone. *Tetrahedron Lett.* **1994**, *35*, 4461–4464. [CrossRef]

72. Lajunen, M.K.; Maunula, T.; Koskinen, A.M.P. Co(II) Catalysed Oxidation of α-Pinene by Molecular Oxygen. Part 2. *Tetrahedron* **2000**, *56*, 8167–8171. [CrossRef]

73. Lajunen, M.K.; Myllykoski, M.; Asikkala, J. Co(II)-catalysed oxidation of α-pinene by molecular oxygen. *J. Mol. Catal. A* **2003**, *198*, 223–229. [CrossRef]

74. Menini, L.; Pereira, M.C.; Parreira, L.A.; Fabris, J.D.; Gusevskaya, E.V. Cobalt- and manganese-substituted ferrites as efficient single-site heterogeneous catalysts for aerobic oxidation of monoterpenic alkenes under solvent-free conditions. *J. Catal.* **2008**, *254*, 355–364. [CrossRef]

75. Maksimchuk, N.V.; Melgunov, M.S.; Chesalov, Y.A.; Mrowiec-Białoń, J.; Jarzębski, A.B.; Kholdeeva, O.A. AEROBIC OXIDATIONS of α-pinene over cobalt-substituted polyoxometalate supported on amino-modified mesoporous silicates. *J. Catal.* **2007**, *246*, 241–248. [CrossRef]

76. Robles-Dutenhefner, P.A.; Da Silva Rocha, K.A.; Sousa, E.M.B.; Gusevskaya, E.V. Cobalt-catalyzed oxidation of terpenes: Co-MCM-41 as an efficient shape-selective heterogeneous catalyst for aerobic oxidation of isolongifolene under solvent-free conditions. *J. Catal.* **2009**, *265*, 72–79. [CrossRef]

77. Li, J.; Li, Z.; Zi, G.; Yao, Z.; Luo, Z.; Wang, Y.; Xue, D.; Wang, B.; Wang, J. Synthesis, characterizations and catalytic allylic oxidation of limonene to carvone of cobalt doped mesoporous silica templated by reed leaves. *Catal. Commun.* **2015**, *59*, 233–237. [CrossRef]

78. Islam, M.; Hossain, D.; Mondal, P.; Roy, A.S.; Mondal, S.; Mobarak, M. Selective oxidation of olefins catalyzed by polymer-anchored nickel(II) complex in water medium. *Bull. Korean Chem. Soc.* **2010**, *31*, 3765–3770. [CrossRef]

79. Sun, X.; Zhao, X.; Jiang, Y.; Xu, B. Synthesis of (−)-3-Carene-2,5-dione via Allylic Oxidation of (+)-3-Carene. *J. Chin. Chem. Soc.* **2013**, *60*, 103–107. [CrossRef]

80. García-Cabeza, A.L.; Marín-Barrios, R.; Moreno-Dorado, F.J.; Ortega, M.J.; Massanet, G.M.; Guerra, F.M. Allylic Oxidation of Alkenes Catalyzed by a Copper–Aluminum Mixed Oxide. *Org. Lett.* **2014**, *16*, 1598–1601. [CrossRef] [PubMed]

81. Hartmann, M.; Kevan, L. Transition-Metal Ions in Aluminophosphate and Silicoaluminophosphate Molecular Sieves: Location, Interaction with Adsorbates and Catalytic Properties. *Chem. Rev.* **1999**, *99*, 635–664. [CrossRef] [PubMed]

82. Timofeeva, M.N.; Hasan, Z.; Panchenko, V.N.; Prosvirin, I.P.; Jhung, S.H. Vanadium-containing nickel phosphate molecular sieves as catalysts for α-pinene oxidation with molecular oxygen: A study of the effect of vanadium content on activity and selectivity. *J. Mol. Catal. A* **2012**, *363*, 328–334. [CrossRef]

83. Cánepa, A.L.; Chanquía, C.M.; Vaschetti, V.M.; Eimer, G.A.; Casuscelli, S.G. Biomass toward fine chemical products: Oxidation of α-pinene over sieves nanostructured modified with vanadium. *J. Mol. Catal. A* **2015**, *404*, 65–73. [CrossRef]

84. Desai, N.C.; Chudasama, J.A.; Patel, B.Y.; Jadeja, K.A.; Karkar, T.J.; Mehta, J.P.; Godhani, D.R. Catalysis by the entangled complexes in matrix structure of zeolite-Y over α-pinene. *Microporous Mesoporous Mater.* **2017**, *242*, 245–255. [CrossRef]

85. Casuscelli, S.G.; Eimer, G.A.; Canepa, A.; Heredia, A.C.; Poncio, C.E.; Crivello, M.E.; Perez, C.F.; Aguilar, A.; Herrero, E.R. Ti-MCM-41 as catalyst for α-pinene oxidation: Study of the effect of Ti content and H_2O_2 addition on activity and selectivity. *Catal. Today* **2008**, *133*, 678–683. [CrossRef]

86. Astruc, D. *Nanoparticles and Catalysis*; Wiley-VCH Verlag GmbH & Co. KGaA: Weinheim, Germany, 2008.

87. Lei, J.; Lu, X.-H.; Zhang, J.-L.; Wei, X.-L.; Zhou, D.; Xia, Q.-H. Epoxidation of mixed bioolefins with air over nanosized Co_3O_4 assisted by ultrasonic waves. *Indian J. Chem.* **2013**, *52A*, 709–716.

88. Genin, E.; Michelet, V. Water as Solvent and Solvent-free Reactions. In *Green Process Engineering. From Concepts to Industrial Applications*; Martine, P., Patrick, C., Gourdon, C., Eds.; CRC Press: New York, NY, USA, 2015; pp. 292–324.

89. Simon, M.-O.; Li, C.-J. Green chemistry oriented organic synthesis in water. *Chem. Soc. Rev.* **2012**, *41*, 1415–1427. [CrossRef]

90. Rauchdi, M.; Ait Ali, M.; Roucoux, A.; Denicourt-Nowicki, A. Novel access to verbenone via ruthenium nanoparticles-catalyzed oxidation of -pinene in neat water. *Appl. Catal. A* **2018**, *550*, 266–273. [CrossRef]

91. Zviely, M. Molecule of the month: Nootkatone. *Perfum. Flavorist* **2009**, *34*, 20–22.

92. Jordan, R.A.; Schulze, T.L.; Dolan, M.C. Efficacy of plant-derived and synthetic compounds on clothing as repellents against *Ixodes scapularis* and *Amblyomma americanum*. *J. Med. Entomol.* **2012**, *49*, 101–106. [CrossRef] [PubMed]

93. Silvestre, A.J.D.; Gandini, A. *Monomers, Polymers and Composites from Renewable Resources*; Belgacem, M.N., Gandini, A., Eds.; Elsevier: Oxford, UK, 2008.

94. Marín, F.R.; Soler-Rivas, C.; Benavente-García, O.; Castillo, J.; Pérez-Alvarez, J.A. By-products from different citrus processes as a source of customized functional fibers. *Food Chem.* **2007**, *100*, 736–741. [CrossRef]

95. Corma, A.; Iborra, S.; Velty, A. Chemical Routes for the Transformation of Biomass into Chemicals. *Chem. Rev.* **2007**, *107*, 2411–2502. [CrossRef] [PubMed]